University of South Bohemia in České Budějovice
Faculty of Science

Subgenomic flaviviral RNA and its role in host cells

Master thesis

Bc. Hana Pejšová

Supervisor: RNDr. Martin Selinger, Ph.D.

České Budějovice 2020

Master thesis

Pejšová H., 2020: Subgenomic flaviviral RNA and its role in host cells. Mgr. Thesis, in English – 75 p., Faculty of Science, University of South Bohemia, České Budějovice, Czech Republic.

Annotation

The aim of this thesis was to determine the functions of subgenomic flaviviral RNA (sfRNA) in host cells. In more detail, sfRNAs derived from dengue virus, zika virus and tick-borne encephalitis virus were studied. Firstly, the impact of sfRNA on *de novo* synthesis of host proteins and rRNA was examined using Click chemistry. Secondly, methodology of sfRNA localisation in host cells was optimised using fluorescence *in situ* hybridisation.

Sworn declaration

I hereby declare that I worked on this Master thesis independently and used only the sources listed in the bibliography.

I hereby declare that, in accordance with Article 47b of Act No. 111/1998 in the valid wording, I agree to the publication of this Master thesis in full in electronic form on the publicly accessible web page of the STAG database operated by University of South Bohemia in České Budějovice, the copyright of this thesis text being retained. I further agree to the electronic publication of the supervisor's and the opponent's assessments of this thesis as well as the electronic publication of the record of the proceedings and the result of this thesis defence in accordance with the above mentioned Act No. 111/1998.

I also agree to the comparison of the text of my thesis with the Theses.cz database operated by the National Registry of University Theses and with a plagiarism detection system.

České Budějovice, 9. 12. 2020 …….

Bc. Hana Pejšová

Acknowledgements

Throughout the working on this thesis, I have received a great deal of support and assistance.

Firstly, I would like to express my deepest gratitude to my thesis supervisor RNDr. Martin Selinger. PhD., whose thorough tutoring was invaluable. I am sincerely grateful for every question answered and every mistake corrected because it pushed me to better myself. Thank you for all your valuable advices and all of the time you have taken from your own work to teach me.

I would like to also acknowledge everyone in the laboratory, who was in any way kind to help and answer my basic questions. Thank you all as I could not have better colleagues than you. Namely, RNDr. Ján Štěrba, PhD., Mgr. Hana Tykalová, RNDr. Pavlína Věchtová, PhD., Mgr. Pavlína Kočová, Mgr. Hana Mašková and Mgr. Libor Hejduk.

Finally, my biggest thank goes to my parents for supporting me in my studies and always having my back when I needed them. This thesis would not exist without you and I am forever grateful to you for being where I am right now.

Contents

1. Preface

Flaviviruses form a diverse group of viruses, many of which are emerging human pathogens and global health threats. Several members of the *Flavivirus* genus cause severe outbreaks with tens of millions of people affected every year (Mackenzie *et al.*, 2004). Many members of flaviviruses such as West Nile virus, yellow fever virus and dengue virus are medically important, however, tick-borne encephalitis virus is one of the most dangerous causative agents of neuroinfections concerning Europe and Asia.

Flaviviruses share a similar genome organisation and apart from its role in the translation of the flaviviral proteins, the genomic RNA was recently observed to generate a small subgenomic RNA species, termed sfRNA. The production of this 0.3 kb to 0.5 kb long RNA was confirmed in all arthropod-borne flaviviruses tested to date (reviewed by Slonchak and Khromykh, 2018). The mechanism by which sfRNA is produced in both mammalian and arthropod cells, is a result of complex conserved secondary structures found in the 3' terminal region of the genome (MacFadden *et al.*, 2018). These complex sequences further undergo incomplete degradation by host cell mRNA decay machinery (Pijlman *et al.*, 2008).

sfRNA acquires several functions which has not yet been fully understood. It potentially plays a part in modulation of host immune response and enhancement of flaviviral pathogenicity. In more detail, it has been confirmed to suppress the type I interferon response in vertebrates (Schuessler *et al.*, 2012) and retroactively inhibit host mRNA degradation pathways (Moon *et al.*, 2012). Understanding the role of sfRNA during flaviviral infection could possibly lead to discovering novel approaches for antiviral treatment and vaccine development.

2. Introduction

2.1 Flaviviruses

Flaviviruses are members of the *Flaviviridae* family which presently comprises of four genera – *Flavivirus, Pestivirus* (*e.g.,* classical swine fever virus and border disease virus), *Hepacivirus* (*e.g.,* hepatitis C virus; Lefkowitz *et al.,* 2017) and *Pegivirus* (Lindenbach *et al.,* 2013). All flaviviruses are important viral pathogens which are considered a world-wide threat with high mortality rates.

The *Flavivirus* genus belongs to arthropod-borne viruses (arboviruses) and is further divided into four ecological groups with more than 70 related viruses – mosquito-borne flaviviruses (MBFs), tick-borne flaviviruses (TBFs), insect-specific flaviviruses and no-known-vector flaviviruses (Kuno *et al.,* 1998). Generally, arboviruses sustain a dual-host tropism as they maintain a transmission cycle between hematophagous arthropod vectors and vertebrate hosts. Insect-specific flaviviruses are exclusively restricted to replicate in arthropod populations (Elrefaey *et al.,* 2020). As stated above, flaviviruses are closely related mainly because they share a similar gene organisation and conserved non-structural protein patterns. However, they differ in amino acid variations and in the cis-acting RNA regulatory elements located at their 5' and 3' ends. Flaviviruses share a common epitope on the envelope protein which results in cross-reactive reactions in serological tests and thus makes diagnostics sometimes difficult (Gubler, 1998).

Moreover, flaviviruses fundamentally differ in distribution, form of transmission and disease manifestation (Gaunt *et al.*, 2001). The pathogenesis of flaviviral infection can vary from an asymptomatic infection or a flu-like illness to jaundice, encephalitis and haemorrhagic disease. Some of the viruses in this genus are medically more known and studied, as they are spread all around the globe, cause multiple outbreaks or have high mortality rate. The genus currently contains 73 viruses, which are classified as 53 species, for example - yellow fever virus (YFV), Japanese encephalitis virus (JEV), West Nile virus (WNV), Murray Valley encephalitis virus (MVEV), zika virus (ZIKV), langat virus (LGTV), tick-borne encephalitis virus (TBEV) and four dengue viruses (DENV; Lindenbach *et al.,* 2013). There is a vaccine available against some of these flaviviruses (YFV, TBEV, JEV; Barrett and Teuwen, 2009) or there are promising candidates in clinical trials (DENV; Troost and Smit, 2020).

Additionally, there are yet no antiviral therapeutics approved for treatment, however, there are many potential drug candidates targeting both viral and host cellular functions (Boldescu *et al.*, 2017; Zakaria *et al.*, 2018, Barrows *et al.*, 2018).

2.1.1 *Virion structure and genome organisation*

All flaviviruses share a similar virion structure which is well characterized especially for DENV and ZIKV (Lindenbach *et al.*, 2013). Mature flaviviral virions are enveloped and roughly spherical particles about 50 nm in diameter (60 nm when immature) and are composed of an electron dense core which is surrounded by a lipid bilayer. The most outer membrane layer of the virion is composed of a glycoprotein coat made of 180 repeating units of large envelope protein (E protein) combined with small membrane protein (M protein; Kuhn *et al*, 2002). The structure differences between a mature and immature virion can be seen in Figure 1.

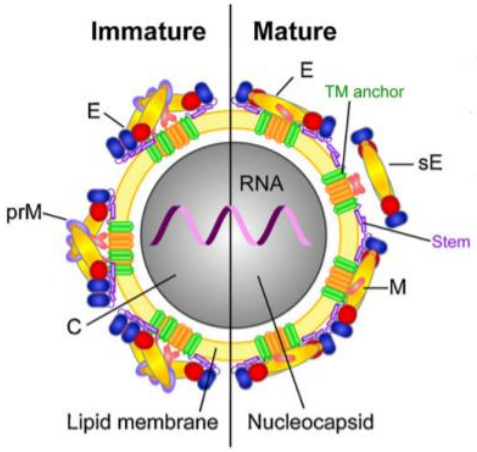

Figure 1: Flavivirus virion structure immature vs. mature (taken from Heinz and Stiasny, 2011).

In contrast, immature virions located intracellularly contain a precursor M protein (prM), which undergoes cleavage to M protein during the exit of the maturing virions from the cell. The surface of the membrane shows icosahedral symmetry (Therkelsen *et al.*, 2018) and the E protein structures are highly dynamic and heterogenic, which results in the breathing of the virion (Kuhn *et al.*, 2015). The viral breathing can be influenced by both viral and environmental genetic factors. More importantly, breathing of the membrane plays a significant role during virion-receptor binding interactions (Meertens *et al.*, 2012).

The genomic RNA (gRNA), located in the core of the virion, consists of a single stranded RNA of positive polarity (approximately 10-11 kb in length). Additionally, the single copy of the genome is complexed with multiple copies of the capsid protein (C protein) which together forms a ribonucleoprotein (Lindenbach and Rice, 2003). The ribonucleoprotein consists of several hundred copies of protein C, which is a 12 kDa dimeric protein with asymmetric charge distribution. The positively charged part of the C protein binds with the gRNA and the nonpolar part interacts with viral envelope (Ma *et al.*, 2004).

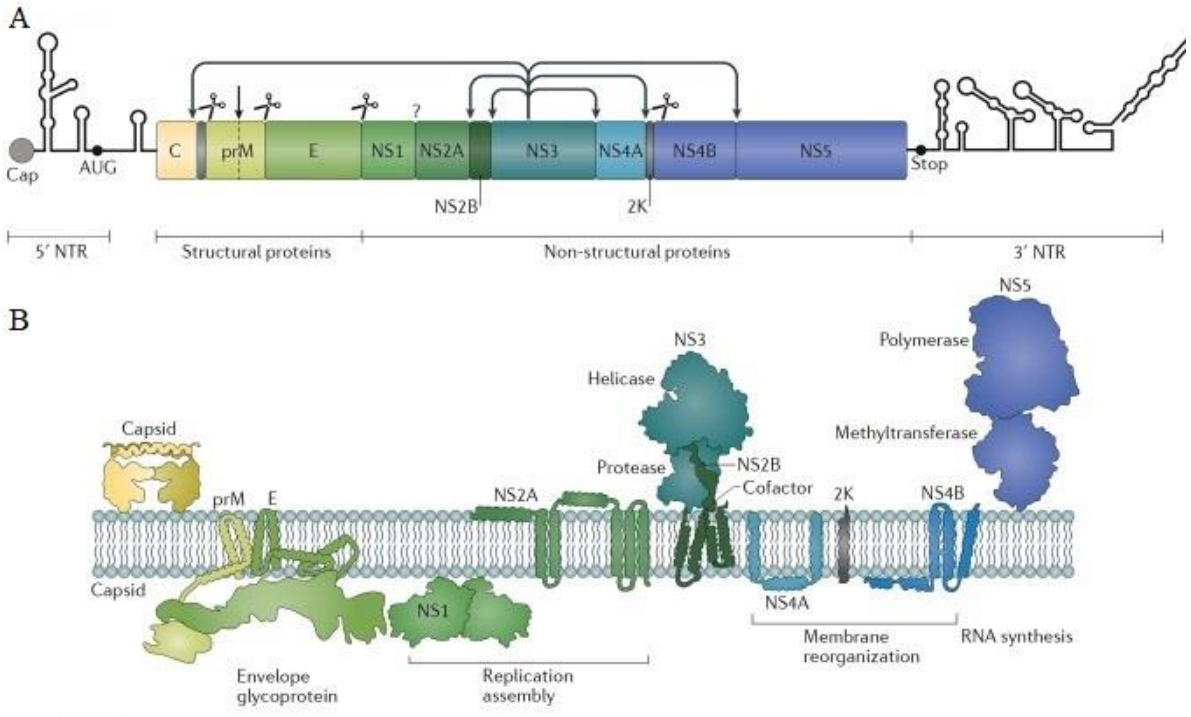

Figure 2: A) Flaviviral genome organisation. B) Flaviviral polyprotein organisation (taken from Neufeldt *et al.*, 2018).

The gRNA is shown in Figure 2 and consists of one open reading frame (ORF) and encodes a single polyprotein (about 3,400 amino acids) which is co- and post-translationally cleaved into three structural proteins (C, prM and E) – and seven non-structural proteins (NS1, NS2A, NS2B, NS3, NS4A, NS4B and NS5; Chambers *et al.*, 1990). The ORF is flanked by 5’ and 3’ non-coding regions and is labeled by a 5’- cap but lacks a 3’- poly(A) tail (Brinton *et al.*, 1986; Ray *et al.*, 2006).

The structural proteins form the virion and the non-structural proteins ensure viral RNA replication, viral polyprotein cleavage, assembly of the virion and interactions with the host

immune system (Roby *et al.*, 2015). Additionally, structural proteins were shown to be important for the virus infectivity and also determine non-viraemic transmission efficiency between co-feeding ticks on a naive animal. The function of prM is most likely to prevent low pH-triggered fusion of the immature virion during exocytosis (Heinz and Allison, 2003). The E protein plays a significant part in pathogenicity of the virion as it interacts with cell receptors and initiates virus-cell membrane fusion. It also has a key role in inducing virus-neutralizing antibodies in mammalian hosts thus functions as an antigen (Heinz, 1986; Mandl *et al.*, 1989). The non-structural proteins were determined to have a serious impact on the cytopathic effect of the virus on the host cells (Khasnatinov *et al.*, 2016).

Generally, the non-structural proteins play an essential role in the viral replication process. During infection, the NS1 protein is localised in the lumen of the endoplasmic reticulum (ER) and associates with the replication complex, but the mechanism by which it is related to the viral RNA synthesis is still unclear (Barrows *et al.*, 2018). NS2A is a small hydrophobic protein (Mackenzie *et al.*, 1998) which specifically binds to the 3' untranslated region (UTR) of viral RNA as well as to prM, E, NS2B and NS3 (Zhang *et al.*, 2019). It plays a significant role in modulating the host antiviral interferon response and the assembly of virus particles. NS2B forms a NS2B-NS3 complex which is required for the cleavage of the viral polyprotein at the ER membrane (Wichapong *et al.*, 2010). NS3 is the second largest flaviviral protein and it possesses three enzymatic activities. Protease activity participates in the maturation of viral proteins, 5' RNA triphosphatase activity is vital for RNA capping by NS5 and helicase activity is necessary for the replication. Both NS4A and NS4B are also components of the replication complex (Welsch *et al.*, 2009). Finally, NS5 is the largest non-structural flaviviral protein and, most importantly, harbours two significant activities: the RNA-dependent RNA polymerase activity (Choi *et al.*, 2004) and RNA methyl-transferase activity (Ray *et al.*, 2006).

The presence of highly structured UTR's at both 5' and 3' terminal ends is vital for viral genome replications and polyprotein translation. The 5' UTR consists of approximately 100 nt and the 3'UTR is composed of approximately 400-700 nt (Rice *et al.*, 1985). The 5' UTR contains two domains which both acquire essential functions. The first domain contains a promoter which is structured as a branched stem-loop (SL; Filomantori *et al.*, 2006) and a uridine-rich region which functions as a spacer and enhances viral replication (Lodeiro *et*

al., 2008). The second domain is composed of a SL structure, a hair-pin structure, a pseudoknot (PK) and a cyclization sequence, which are all essential in viral RNA replication. More interestingly, some of these sequences directly interact with corresponding structures in the 3'UTR (Gebhard *et al.*, 2011).

The 3'UTR contains three distinctive domains. The first domain is the least conserved and is referred to as the variable region. Additionally, it contains two SL structures (SL I and SL II) which form two PKs. These sequences of the RNA are exonuclease-resistant and result in the formation of subgenomic flaviviral RNA (sfRNA). The second 3'UTR domain contains either one or two conserved dumbbell structures (DB), which form up to two additional PK's for the production of sfRNA. Notably, these sequences are also essential for the pathogenesis of the virus, viral replication and protein synthesis. Lastly, the third domain of the region is highly conserved and contains interaction sites to inverted complementary sequences localised in the 5'UTR which result in the circularization of the flaviviral genome (Manzano *et al.*, 2011; Friebe *et al*, 2012).

In all flaviviruses, there are several RNA modifications which the gRNA undergoes and which are critical for the infection of the host. Firstly, the 5' end of the genome is methylated by both viral and host enzymes. The generated RNA transcript is modified by the addition of 2'-O-methyl group to the penultimate nucleotide on the 5' terminal end which yields a type I cap (Wei *et al*., 1975). Secondly, other type of modification of flaviviral RNA is internal adenosine methylation, for example within the coding region of NS5 (Gokhale *et al*, 2016). These RNA modifications are a highly promising candidates for vaccine strains because recombinant flaviviruses lacking 2'-O-methyltransferase enzymatic activity are attenuated and provide protection against an infection with virulent viruses (Zust *et al.*, 2013).

2.1.2 *Flaviviral life cycle*

In the first stage of the flaviviral life cycle, the virion binds to the cell surface via interaction of the viral glycoprotein E and a receptor on the cell membrane (Figure 3). It is still not clear which molecules act as receptors but it is hypothesized that heparan sulfate could be the potential candidate to mediate the binding, presumably because it is abundantly found on the surface of both vertebrate and tick cells (Chen *et al.*, 1997; Mandl *et al.*, 2001). So far, the only receptors which were identified as attachment factors in mosquito and mammalian cells are for

DENV and include DC-SIGN and heat-shock family proteins (Salas-Benito *et al.*, 1997, 2007). Following the attachment to the membrane, receptor-mediated endocytosis via clathrin-coated pits is initiated and the virion entries the cell in an endosomal vesicle. Subsequently, the acidic pH in the endosome results in the spontaneous fusion of the virion and the endosomal membrane and the viral nucleocapsid is eventually released into the host cell's cytoplasm (Mackenzie, 2005).

The mechanism by which the ribonucleoprotein is disassembled in the cytoplasm is still not clear, but the C protein is proposedly released from the gRNA by elongating ribosomes (Garcia-Blanco *et al*, 2016). The positive sense gRNA can be used for both protein translation and generation of a negative-sense template for viral replication (Sotcheff and Routh, 2020).

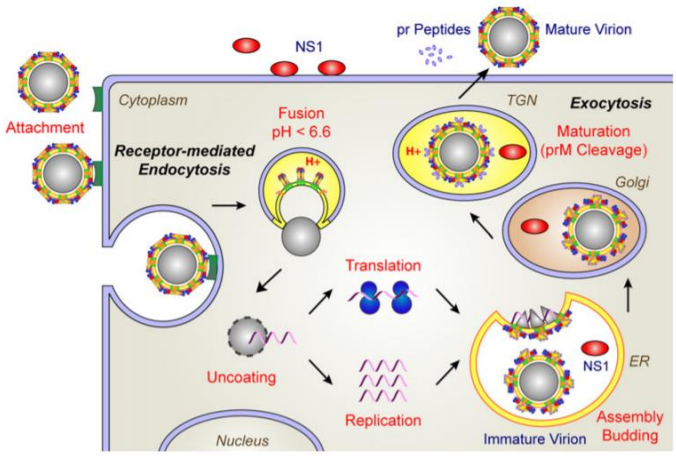

Figure 3: Schematic representation of flavivirus life cycle (taken from Heinz and Stiasny, 2011).

When the gRNA is released from the endosome, it undergoes translation at ribosomes to yield the viral polyprotein which is co- and post-translationally cleaved by viral protease (NS2B-NS3 protease) as well as cellular proteases (signalase and furin). The cleavage as well as the replication of the viral genome is located at specialized sites at the ER and the double membrane vesicle packets derived from the Golgi-apparatus (Mackenzie, 2005). The translation begins in the cytosol after the recruitment of 40S and 60S ribosomal subunits and associated factors but the entire complex is then delivered to the translocon in the ER membrane (Barrows *et al.*, 2018). Alternatively, the flaviviral genome can be recruited to the ER before the translation is initiated (Reid *et al.*, 2015).

The positive strand viral genome also functions as a template for the production of new genomes. The replication requires both viral proteins and additional cellular factors. Furthermore,

the synthesis of viral RNA depends upon the rearrangements of intracellular membranes (virus-induced invaginations of the ER) of infected cells (McGavran and White, 1964) and is provided by replication complex which is composed of viral non-structural proteins as well as cellular components (Shi, 2014).

After the translation of the polyprotein and the synthesis of new RNA genomes is completed, the C proteins are situated on the cytoplasmic side of the ER. Subsequently, they capture the newly synthesized genomes to form a nucleocapsid complex on the cytoplasmic site of the ER and this ribonucleoprotein complex is internalized into the ER lumen, which allows it to acquire a lipid membrane. The lipid membrane is additionally anchored with viral structural proteins prM and E and the whole particle then forms an immature virion (Tan *et al.*, 2020). Consisting of the three structural proteins, C, prM and E, immature and non-infectious virions are assembled in the neutral pH inside the endoplasmic reticulum. These particles have protomers of prM/E which interact together and these interactions result in a formation of spiky particles exposing the viral membrane and showing icosahedral symmetry (Rey *et al.*, 2017). These immature virions are exposed during exocytosis to the acidic milieu of the trans Golgi apparatus network which leads to the conformational re-organisation of the protomers into 90 $(prM/E)_2$ dimers, which form a different glycoprotein shell, resulting in complete coating of the viral membrane. In more detail, these immature particles are transported through the secretory pathway and furin-mediated proteolysis of prM in the trans Golgi network leads to rearrangement of prM-E complex. The pr fragment is separated from the rest of the M protein in the neutral pH milieu and this final modification results in maturation of the fully infectious virions which are eventually secreted out of the cell (Yu at al., 2008). Secreted mature virions are accompanied by partially matured and immatures ones, but only the mature and partially mature particles are capable of fusion with adjacent host cell and thus be infectious (Pulkkinen *et al.*, 2018).

Flaviviruses infect a various number of cells including monocytes, macrophages, dendritic cells, neurons *etc.* (Marianneau *et al.*, 1999; Tassaneetrithep *et al.*, 2003; Hirano *et al.*, 2014). Generally, the transmission of the virus occurs in the site of the bite of the vector and the virus then replicates in the local tissues. Following the initial replication, the virus migrates via draining lymph nodes where it further replicates in monocyte lineage cells (macrophages, dendritic cells or microglial cells). These virus-infected cells then migrate and cause primary viraemia which

simultaneously results in infection of peripheral organs such as spleen and kidneys. In the case of neurotropic flaviviruses, the virus subsequently enters blood circulation, crosses the blood-brain barrier (BBB) and invades the central nervous system. The capability to cross the BBB is a vital factor for the pathogenesis of neurotropic flaviviruses such as TBEV and JEV, however, the mechanism is still unclear (Ye *et al.*, 2013).

2.1.3 *Members of the Flavivirus genus*

As mentioned above, the *Flavivirus* genus contains more than 70 viruses. For the purposes of this thesis, only flaviviruses used for experiments are discussed in more detail.

2.1.3.1 Tick-borne encephalitis virus

Tick-borne encephalitis virus is considered the causative agent of one of the most important tick-borne infections called tick-borne encephalitis (TBE). In Europe and North Asia, there are approximately 5,000-13,000 cases reported annually (Lindquist and Vapalahti, 2008). However, the number could be potentially higher as many mild infections go undiagnosed. Most of the cases occur from April to November, because ticks are most active during these warm months. The TBEV serocomplex is further divided into three sub-types, namely Far Eastern subtype (previously referred to as Russian Spring-Summer Encephalitis), Siberian subtype and European subtype (previously referred to as Central European Encephalitis, Ecker *et al.*, 1999). However, there are many viruses in Europe, Asia, and Canada which are antigenically related to TBEV and they are considered as a TBEV serocomplex (known as Mammalian group of TBFs – Omsk haemorrhagic fever virus, louping ill virus, powassan virus, LGTV *etc*. TBEV cannot be found in the tropics and subtropics but it is an increasing danger in many parts of Europe, Russia, and the United States of America. Naturally, the virus circulates between tick vectors (*i.e*., *Ixodes ricinus* in Europe, *I. persulcatus* in Asia, and *I. scapularis* in North America) and vertebrate hosts (Burke and Monath, 2001).

2.1.3.1.1 Transmission of TBEV

Transmission of TBEV generally occurs in three different mechanisms. Commonly, in tick-infested areas in Asia and Europe, the reservoirs of the virus are viraemic vertebrates such as small rodents, deer, moles, hedgehogs *etc*., which then serve as the source of the virus for ticks. Adult ticks and nymphs become infected during feeding on the viraemic animal and the virus reproduces in them. During feeding of ixodid ticks, their salivary glands undergo extensive

development and most of the fluid which is ingested by the tick is later excreted back into the host via regurgitation (Bowman *et al.*, 2008). In the final stages of its reproduction cycle in the vector, the virus is eventually transported from the midgut via hemocoel to salivary glands, from which it is then transmitted via saliva to other animals as the tick takes its next meal (Gritsun *et al.*, 2003). The mechanism by which the virus exits hemocoel and reaches tick salivary glands is still unclear (Kaufmann and Nuttall, 1996). Infected ticks can naturally fast up to a year before their next feeding. However, the infectivity rate of TBEV in female ticks after a bloodmeal is higher than in ticks which were fasting for a prolonged period of time (Slovak *et al.*, 2014). The reason for that could potentially be a self-protection mechanism to preserve the function of salivary glands when ticks are fasting (Bowman *et al.*, 2008.)

Secondly, the replication of TBEV in the early stages of the infection occurs also in the skin. Thus, an interesting case of transmission takes place during co-feeding of two or more different ticks on the same host at the same time. It is called non-viraemic transmission because it is not essential to develop viraemia for the infection in the vertebrate animal, it is more likely a secondary product of this process. The animal can be susceptible, insusceptible as well as immune to the infection, which makes this mode of transmission highly efficient (Labuda *et al.*, 1996; Labuda *et al.*, 1997). The vehicles for TBEV during this co-feeding type of transmission could potentially be Langerhans cells (skin Langerhans cells are members of the dendritic cell system) and keratinocytes at the local skin site. In detail, epidermal dendritic cells internalize foreign antigens, express the relevant MHC molecules and then migrate to draining lymph nodes to deliver information for T cells activation. This transport system could be possibly the main dissemination vehicle of the virus inside the host (Labuda *et al.*, 1996).

Lastly, the third possible model of spreading is provided only by the tick vector. This mechanism known as vertical transmission of the virus originates from infected female adult ticks which pass the virus to their eggs and larvae. It is called transovarial transmission and it occurs very rarely (Rehacek, 1962; Singh *et al.*, 1963). It has been demonstrated that the infection rate of *I. ricinus* larvae matured from TBEV-positive eggs is below 1% (Danielová and Holubová, 1991).

Humans usually acquire the infection by the bite of an infected adult tick. However, in rare cases, the transmission of the virus is possible by the consumption of unpasteurized milk or other dairy products from goats and sheep (Burke and Monath, 2001).

2.1.3.1.2 TBE manifestation and pathology

The incubation period of the virus in humans is between 7 to 14 days and the first phase can be misinterpreted for an influenza-like illness. In general, the severity of the disease increases with the age of the patient. Most common symptoms are headache, fever, muscle pain and fatigue. After these symptoms disappear, one third of the patients further develop the second phase with neurological symptoms. There are several forms which differ in the severity of the neuroinfection: meningeal, meningoencephalitic, poliomyelitic and polyradiculoneuritic (Gritsun at al., 2003). Interestingly, chronic forms of the disease have also been reported but only in Siberia and Far East Russia. In addition, the fatality rates are also significantly higher in these parts of Russia which could indicate that these strains are more virulent.

Similar to other flavivirus infections, the primary cells utilized by TBEV for infection are epidermal Langerhans cells (Chambers and Diamond, 2003). As a vehicle, these cells transport the virus to the draining lymph nodes which results in the spread of the infection to other tissues. The mechanism by which the virus reaches the brain has not yet been fully cleared, but it presumably involves either infection of endothelial cells (Mandl, 2005) or a leukocyte-mediated transport (Miner and Diamond, 2016). During the ongoing infection in the host body, neurons are primary targets of TBEV (Hirano *et al.*, 2014), but other brain cells were confirmed to be infrequently sensitive to the virus as well (Potokar *et al.*, 2014). It was suggested that the infection of glial cells may potentially increase the pathogenic effect of the viral replication. In more detail, the replication of TBEV in glial cells is essential to the efficient spreading of the infection throughout the brain. Moreover, glial cells play a significant role of producing a high rate of immune mediators (cytokines and chemokines) such as IL-1β, IL-6, IL-8, IL-10, IFNα, TNF-α; Verma *et al.*, 2010). The excessive production of these mediators may influence the balance between adequate immune reaction and neurotoxicity during inflammatory response to the infection. This also corresponds with the fact that the entry of TBEV into the central neural system precedes the eventual disruption of BBB, which is later caused by the overproduction of cytokines and chemokines previously mentioned (Růžek *et al*, 2011).

The infected neural cell undergoes a significant ultrastructural rearrangement of the cytoskeleton as well as other cell organelles such as the rough ER and Golgi apparatus. This allows formation of new compartments in the cytoplasm, which are eventually utilized as functional sites for protein synthesis, RNA replication and generation of novel protection against host immune system (Gillespie *et al.*, 2010; Offerdahl *et al.*, 2012; Miorin *et al.*, 2013). These structures can be seen as convoluted membranes, paracrystalline arrays or membrane sacs containing small vesicles. These vesicles contain a pore opening to the cytosol which allegedly functions as a polyprotein processing site (Welsch *et al*, 2009).

The TBEV infection was confirmed in both human (Palus *et al.*, 2014) and rodent astrocytes with no decrease of the viability of the cells (Potokar *et al.*, 2014). Astrocytes are the most numerous group of glial cells (Nedergaard *et al.*, 2003) and have a number of functions in the brain, including the supply of nutrients to surrounding tissues, repairing and scarring process of damaged cells and support of endothelial cells that form the BBB.

Unfortunately, there is presently no licensed therapeutics available for the treatment of TBE (Lehrer and Holbrook, 2011). Nonetheless, a vaccine commercially called FSME-IMMUN® has been on the market since 1976 and it has provided significant help in the fight against TBEV (Kunz *et al.*, 1976). The immunization against either European subtype or Far eastern subtype of TBEV leads to cross-neutralizing of antibody response and cross-protection given the degree of homology of the E protein amino acid sequence between the vaccine virus strains (Fritz *et al.*, 2012).

2.1.3.2 Dengue virus

Since the first dengue-like infection dated back to AD 265-420 (Nobuchi, 1979), DENV has been described numerous times throughout history and is presently the leading arboviral disease in the world. Additionally, it is considered by WHO as a major global public health threat, particularly in the tropic and subtropic parts of the world. DENV serogroup includes four related but antigenically distinct serotypes (DENV-1, DENV-2, DENV-3, DENV-4; Halstead, 1988).

Unlike TBEV, DENV's only natural hosts are solely mosquitoes, humans, and lower primates with no clinical manifestation (Henchal *et al.*, 1990). The viruses are transmitted to humans by *Aedes aegypti* mosquitoes (Lindenbach *et al.*, 2013) through a penetration of the skin following a bite by an infected mosquito (Gubler *et al.*, 1988). The cycle begins when

a susceptible mosquito takes a meal on an infected host and ingests high enough volume of viral particles (more than 5 $\log_{10}$-copies/ml is sufficient for transmission; Nguyen *et al.*, 2013). During the first ten days of the infection inside the vector, the virus replicates in various tissues and eventually reaches salivary glands (Linthicum *et al*., 1996; Salazar *et al.*, 2007) in a mechanism which is still not clarified (Cao-Lormeau, 2009).

The incubation period in a human host is 3 to 14 days and there are several stages of clinical manifestations distinct in symptoms, severity and mortality. These stages are: undifferentiated fever which frequently goes undiagnosed, Dengue fever, Dengue haemorrhagic fever, which occurs mostly during the secondary infection of other DENV serotype, and eventually Dengue shock syndrome, which leads to multiorgan dysfunction and death (Hasan *et al.*, 2016).

2.1.3.3 Zika virus

Zika virus is a MBF firstly isolated from a rhesus monkey used in a research program for YFV in Kampala, Uganda in 1947 (Dick *et al.*, 1952) and since then it has caused multiple outbreaks. Until 2007, the cases were solely in Asia and Africa, but two major outbreaks occurred in the Pacific Island of Yap and in French Polynesia (Hall, 2017). The most recent outbreak occurred in the American continent in 2015-2016 due to the spreading of the Asian strain of the virus (Hennessey *et al.*, 2016).

The transmission cycle of ZIKV in arthropod vectors shows serological overlapping with other flaviviruses like DENV, WNV (Korhonen *et al.*, 2016) and Chikungunya virus (Christofferson, 2016). There are multiple modes of transmission, however, one of the most frequently occurring is from the bite of an infected mosquito (*A. aegypti* and *A. albopictus*; Ciota *et al.*, 2017). Zika virus was also shown to be able to cross the placental barrier and cause congenital infections as well as be transmitted sexually among humans (Foy *et al*., 2011; Venturi *et al*., 2016), which is very rare to flaviviruses.

Presently, WHO raised awareness of ZIKV infection mostly in economically deprived countries because there are no vaccines or antiviral treatment available for the disease. (Agumadu and Ramphul, 2017).

2.2 Subgenomic flaviviral RNA

As mentioned in the beginning, flaviviral gRNA consists of 5' and 3'UTRs. These UTRs possess vital functions in viral replication cycle, polyprotein translation and virion packaging mechanisms (Markoff, 2003). Apart from these functions, the generation of sfRNA species derived from the 3'UTR has been observed in all flaviviruses tested to date - MVEV (Urosevic *et al.*, 1997) JEV (Lin *et al.*, 2004; Chang *et al.*, 2013), WNV (Scherbik *et al.*, 2006; Pijlman et at., 2008), YFV (Silva *et al.*, 2010) DENV (Schnettler *et al.*, 2012), ZIKV (Akiyama *et al.*, 2016), TBEV and LGTV (Schnettler *et al.*, 2014).

The sfRNA was given immense attention in recent years, because its presence plays a significant role in inducing viral cytopathicity in cell culture and pathogenicity in mice (Pijlman *et al.*, 2008). Since its discovery, experiments have been mostly focused on sfRNA from MBFs such as DENV, YFV, and WNV.

2.2.1 *Mechanism of sfRNA generation*

2.2.1.1 Stalling of exoribonuclease XRN1

Many viruses utilize the machinery of the host cell for their benefit. Flaviviruses adapted a unique mechanism by which a part of their gRNA completely escapes the mRNA decay machinery resulting in the generation of sfRNA. This machinery occurs in conserved structures known as cytoplasmic processing bodies and it plays a significant role in both host and viral mRNA turnover. A key enzyme responsible for processing of decapped single-stranded mRNA is called 5'-3' exoribonuclease XRN1 (Sheth and Parker, 2003). XRN1 is conserved in eukaryotes and it functions as the main cytoplasmic RNase with 5'-3' activity as well as RNA-helicase activity.

However, XRN1 is unable to degrade complex structures in the 3'UTR of the flaviviral genome, which results in the stalling of the exoribonuclease (Pijlman *et al.*, 2008; Funk *et al.*, 2010; Moon *et al.*, 2012). The stalling of XRN1 is primarily due to a short RNA sequence of approximately 80 nt situated at the 5' end of sfRNA (termed SL-E in YFV and SLII in WNV). These sequences, called XRN1-resistant structures (xrRNAs), show high stability and contain strong secondary structures such as several SLs (*i.e.*, SLII in DENV or SL-E in YEF) followed by one or two DB structures and long 3'SL. These secondary structures are uniquely conserved among all flaviviruses demonstrated to produce sfRNA (Pijlman *et al.*, 2008; Liu *et al.*, 2010).

The 5’ end of WNV sfRNA aligns with the SLII structure and disruption of this structure leads to generation of truncated sfRNA species indicating that SLII is vital for the production of complete sfRNA (Pijlman *et al*., 2008). Additionally, three alternative sfRNAs (sfRNA-2, sfRNA-3 and sfRNA-4) were detected in infected cells showing that SLIV and potentially other two DB structures located downstream could also result in the stalling of XRN1 (Pijlman *et al.*, 2008; Funk *et al.*, 2010, Filomatori *et al.*, 2017).

2.2.1.2 Conserved secondary and tertiary structures of xrRNA

Presently, xrRNAs formed by SLs and DBs are the only two forms of xrRNA elements that have been described (Funk *et al.*, 2010). However, the total number of alternative sfRNA species generated in MBFs is variable. For example, YFV shows only one set of xrRNAs with only one SL and one DB (Silva *et al.*, 2010). On the other hand, the majority of MBFs contain duplicated xrRNA elements (Villordo *et al.*, 2016). DENV and WNV have two SLs (SLII and SLIV for WNV and SLI and SLII for DENV) and two DBs (DBI and DBII; Funk *et al.*, 2010; Filomatori *et al.*, 2017). These domains are commonly referred to as xrRNAs 1 to 4 resulting in the production of sfRNAs 1 to 4, respectively (Figure 4).

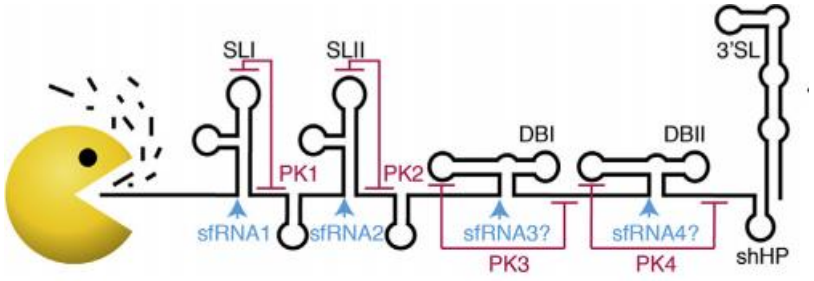

Figure 4: Schematic representation of four sfRNA species in the 3’UTR of DENV (adapted from Slonchak *et al*., 2018).

Firstly, the crystal structures of xrRNA-1 of ZIKV (Akiyama *et al.*, 2016) and xrRNA-2 of MVEV (Chapman *et al.*, 2014) have been described using X-ray crystallography. Both of the analysed xrRNAs form stable three-way junctions with coaxial stacking of helices P1 and P2, where P3 is positioned to P1 in an acute angle (shown in Figure 5). Three-way junctions are common structural elements, forming branches in nucleic acids, found in highly structured RNAs such as rRNA and hammerhead ribozymes (Lilley, 1998). However, a new topology of three-way junctions has been discovered in the case of xrRNAs. This three-way junction has

a knot-like conformation in which the 5'-end of the RNA goes through a ring-like structure (Chapman *et al.*, 2014; Akiyama *et al.*, 2016).

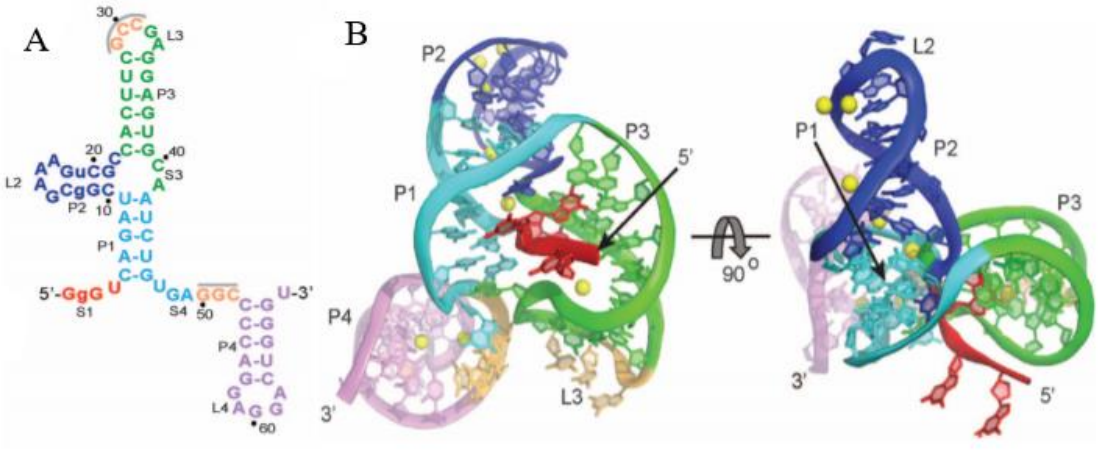

Figure 5: Structure of xrRNA of MVEV. **A**) Crystallised RNA sequence. **B**) Two views of the structure from two different angles coloured to match A). Figures taken from Clarke *et al.*, 2014.

This model presumably indicates that the ring surrounding the 5'end of RNA alters the active site of the exonucleolytic enzyme which subsequently results in the prevention of accessing the following nucleotide and overall blockage of the 5' to 3' degradation progress (Chapman *et al.*, 2014). Formation of the ring-like topology is stabilized by a small PK and base pairing (Watson-Crick and non-canonical) with the junction. PK between the apical loop of xrRNA-forming SL and down-stream complementary region of 3'UTR was not identified in the crystal structure of MVEV xrRNA-2 (Chapman *et al.*, 2014). On the other hand, the PK was clearly evident in the crystal structure of ZIKV xrRNA-1 (Akiyama *et al.*, 2016) which suggests that the presence of PK is not necessary for the formation of xrRNA but it increases its stability (Kieft *et al.*, 2015; Akiyama *et al.*, 2016).

In the case of TBFs, the xrRNA structures were also confirmed to form three-way junctions and PK between apical loop and downstream 3'UTR sequence (Schnettler *et al.*, 2014; MacFadden *et al.*, 2018). However, the position of sfRNA start site was located in a convex region within a longer stem, whereas in MBFs it is located prior to the stem region. The presence of PK in TBFs xrRNA was also shown to be crucial for the sfRNA generation (MacFadden *et al.*, 2018). Unfortunately, the crystal structure of TBFs has not yet been determined.

2.2.2 *Functions of sfRNA*

sfRNA possesses several important functions which lead to an increased cytopathicity in cell cultures as well as pathogenicity in mice (Pijlman *et al.*, 2008). One of the first discovered functions of sfRNA, was the ability to retrospectively repress XRN1 enzymatic activity in both mammalian and arthropod cells (Moon *et al.*, 2012; Chapman *et al.*, 2014). The XRN1 progresses along the gRNA and after its stalling at the xrRNA structure, the release of the enzyme from the proximal side of 3'UTR is slowed or completely prevented. This results not only in promoting the stability of flaviviral RNAs to increase viral replication, but also in the abundant accumulation of uncapped mRNAs and increased stability of host transcripts (Moon *et al.*, 2012).

Secondly, sfRNA was confirmed to suppress RNA interference (RNAi) antiviral response in mosquito and mammalian cells (Moon *et al.*, 2015) as well as tick cells (Schnettler *et al.*, 2012). RNAi is a primary mechanism of innate immune response in invertebrates. The mechanism involves recognition of double-stranded viral RNA by endoribonucleolytic enzyme Dicer which possesses the ability to cleave this RNA into approximately 18-28 nt double-stranded fragments referred to as small interfering RNA. These small RNAs can later prevent translation by directing enzyme complexes against mRNA (Bernstein *et al.*, 2001). The ability to inhibit RNAi indicates that sfRNA has the ability to overcome initial immune defence thus preventing processing of viral gRNA and RNA replication intermediates (Göertz *et al.*, 2018).

The ability of sfRNA to inhibit immune response in vertebrates by altering type I interferon (IFN) response was also discovered. Type I IFN response pathway has been demonstrated as the most important mediator of host resistance to flavivirus infection (Diamond and Gale, 2012). In a nutshell, type I IFNs are pro-inflammatory cytokines whose production is induced following recognition of pathogenic patterns. This immune defence system is highly efficient because type I IFN receptor is expressed in every cell type. These cytokines are produced in infected cells; however, non-infected adjacent cells stimulate production of antiviral factors to prevent viral spreading (Stark *et al.*, 1998). The inhibitory effect of sfRNA on type I IFN response was demonstrated for WNV (Schuessler *et al.*, 2012), DENV-2 (Bidet *et al.*, 2014; Manokaran *et al.*, 2015) and ZIKV (Donald *et al.*, 2016). The mechanism of action which sfRNA molecules use to work against the IFN pathway has not yet been fully determined. It was

suggested that both DENV and ZIKV sfRNAs antagonize retinoic acid-inducible gene I mediated type I IFN response (Manokaran *et al*, 2015; Donald *et al.*, 2016), in which retinoic acid-inducible gene I is a cytosolic pattern recognition receptor responsible for recognizing cells infected with virus and inducing type I IFN response (Bowie and Fitzgerald, 2007).

In conclusion, the importance of fully understanding sfRNA functions is crucial, as its presence during infection strongly boosts flaviviral pathogenicity. Thus, determining other factors could potentially lead to discovering novel pathways of targeting it for antiviral treatment or vaccine manufacturing.

3. Aims and objectives

- Optimisation of cell transfection with *in vitro* transcribed sfRNA.
- Determination of the role of sfRNA on *de novo* host protein synthesis.
- Determination of the role of sfRNA on *de novo* host rRNA transcription.
- Localisation of sfRNA in transfected and infected cells using fluorescence *in situ* hybridization.

4. Materials and methods

4.1 Plasmids

Two strains of the West-European TBEV subtype were chosen for the purposes of this thesis, each with a different degree of virulence – medium Neudoerfl (GenBank accession no. U27495) and severe Hypr (GenBank accession no. U39292). Additionally, two MBFs were also selected for experiments to show the comparison between TBFs and MBFs – ZIKV strain PE243 (GenBank accession no. MF352141) and DENV-2 (GenBank accession no. M19197).

3'UTRs of these strains (containing sfRNA sequences) were cloned into Gateway® pcDNA™ DEST40 plasmids (Invitrogen) containing CMV and T7 promotors and HDVr (hepatitis delta virus ribozyme). The presence of HDVr element is crucial for the generation of desired RNA molecules of precise length using T7 *in vitro* transfection. The elements contained in pDEST40 plasmid can be seen in Figure 6.

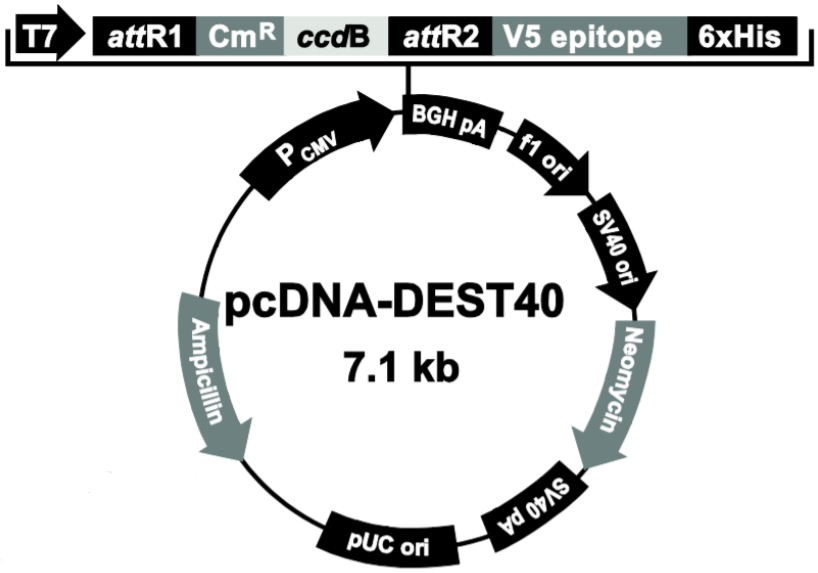

Figure 6: Map and features of pcDNA™-DEST40 (adapted from Invitrogen Gateway® pcDNA-DEST40 Vector User Guide).

The Neudoerfl 3'UTR construct used in our experiments was adapted from Schnettler *et al*., 2014. Hypr 3'UTR construct was prepared in our laboratory. DENV-2 3'UTR containing plasmid was adapted from Schnettler *et al*., 2012. Lastly, ZIKV 3'UTR cloned into pDEST40 vector was constructed by Donald *et al*., 2016.

For all experiments, a pDEST40 construct with incorporated maltose-binding protein (MBP), a gene of bacterial origin, was used as a negative control. MBP coding sequence was also fused to HDVr (Schnettler *et al*., 2012).

4.2 *In vitro* transcription of sfRNA (DENV, ZIKV, TBEV Hypr and Neudoerfl strain)

For all experiments, *in vitro* transcribed sfRNA of DENV, ZIKV, TBEV (Hypr and Neudoerfl strains) sfRNA was prepared using pDEST40 plasmids containing the 3'UTRs. The following mix of components was added according to the manufacturer's protocol (MEGAscript™ T7 Kit) – 2 µl of ATP, GTP, UTP, CTP; 2 µl 10× reaction buffer; 2 µl of T7 Enzyme mix; 1.5 µg of non-linearized plasmid of each 3'UTR; RNase-free H_2O filled to 20 µl. The reactions were subsequently incubated at 37°C for 6 hours.

After the incubation finished, the samples were treated with 1 µl of TURBO DNase and incubated for additional 15 minutes at 37°C. The RNA was then precipitated with 60 µl of LiCl precipitation solution (30 µl LiCl diluted in 30 µl RNase-free H_2O) for at least 30 minutes at -20°C and then centrifuged at 16,500 × g for 30 minutes at 4°C. After the extraction of the supernatant, the RNA pellets were washed with 70% ethanol, centrifuged for additional 5 minutes at the same conditions and then dried on air for 5 minutes. Dried pellets were dissolved in RNase-free H_2O (45 µl) and the concentration of the purified sfRNAs was measured using the NanoPhotometer® (Implen). Obtained RNA samples were stored at -80°C until further use.

4.3 Transfection of DAOY HTB-186 cells with *in vitro* transcribed sfRNA

Human medulloblastoma cell line (DAOY HTB-186) was used for all *in vitro* experiments. This cell line is derived from desmoplastic cerebellar medulloblastoma of a 4-year-old Caucasian male (Jacobsen *et al*., 1985). The cell culture was grown in a DMEM low glucose medium enriched with 10% foetal bovine serum (FBS), 1% L-alanyl-L-glutamine, and 1% antibiotics-antimycotics (Amphotericin B 0.25 µg/ml, Penicillin G 100 units/ml, Streptomycin 100 µg/ml) at 37°C and 5% CO_2.

The cells were seeded one day prior to transfection into 6-well-plates/12-well-plates according to Table I.

Table I: Seeding density and transfecting volumes for 6-well and 12-well plates.

panel	cell density	sfRNA mix		Polyjet mix	
		RNA (µg)	DMEM (µl)	Polyjet (µl)	DMEM (µl)
6-well	5×10^5	1	to 100	3	97
12-well	2.5×10^5	0.75	to 75	2.25	72.75

The following day, cells were transfected with transcribed sfRNA (see 4.2) using Polyjet™ *In vitro* DNA Transfection Reagent (SignaGen Laboratories) according to the manufacturer's protocol. Fresh medium was added to the cells prior to the transfection.

The needed amount of sfRNA and Polyjet (Table I) were separately diluted in low-glucose DMEM medium without serum and other additives, the two reactions were then mixed, incubated at room temperature (RT) for 10-15 minutes and then added drop-wise onto the medium in each well. The transfected cells were then incubated for additional 24 or 48 hours at the same conditions.

In the case of metabolic labelling of proteins, the cells were grown and transfected in RPMI medium.

4.4 Quantitative Real-time PCR of total RNA from transfected DAOY cell line

4.4.1 *RNA isolation*

24 and 48 hours post transfection (hours p.t.), total RNA was isolated using phenol-based RNA Blue reagent (Top-Bio) according to the manufacturer's instructions. In short, the cells were washed with PBS and then 1 ml of RNA Blue reagent was added to each well in a 6-well-plate to lyse the cells for 5 minutes at RT. Afterwards, the lysate was transferred to a new 1.5 ml Eppendorf tube and 0.2 ml of chloroform was added. The samples were thoroughly vortexed for at least 15 s, incubated for 5 minutes at RT and centrifuged at 12,000 × g for 10 minutes at 4°C. Subsequently, the aqueous phase of the samples was transferred into a fresh tube and the RNA was precipitated with 0.5 ml of isopropanol at 4°C overnight. The samples were centrifuged at 16,500 × g for 30 minutes at 4°C, the supernatant was removed and the RNA precipitate was washed with 75% ethanol and centrifuged at the same conditions for additional 10 minutes. Eventually, the supernatant was removed and the pellets were air-dried for 5 minutes and then dissolved in 20 µl RNase-free H_2O. The yielded total RNAs were stored at -80°C.

4.4.2 *Quantitative Real-time PCR*

For real-time qPCR analyses, KAPA SYBR® FAST Universal One-Step qRT-PCR Kit (Roche) was used according to the manufacturer's protocol. The reaction volume for Quantitative Real-time PCR (qRT-PCR) was 15 µl and contained 7.5 µl of 2× Master Mix, forward and reverse primers (ZIKV 200 nM, DENV-2 150 nM, TBEV 150 nM and HPRT 300 nM), 0.3 µl of 50× RT mix, 4 µl of total RNA (10-20 ng/µl) and the remaining volume was adjusted with RNAse/DNAse-free water. The sequences of primers used can be found in Table II.

Table II: List of used primers.

Primer	**Sequence 5' to 3'**	**Source**
TBEV C F	ATGGTCAAGAAGGCCATCCTGAAAG	our laboratory (designed for Hypr)
TBEV C-Hypr R	CCTCCTTTTTCCGCGTTTTTGCAAG	our laboratory (designed for Hypr)
DENV2-F	TTGAGTAAACTATGCAGCCTGTAGCTC	Chien *et al*., 2006
DENV2-R	GGGTCTCCTCTAACCTCTAGTCCT	Chien *et al*., 2006
ZIKV sfRNA F	CCTATAGTCAGGCCGAGAACG	our laboratory
ZIKV sfRNA R	CCACCTTCTTTTCCCATCCTG	our laboratory
TBEV probe sfRNA F	CAGTGAGAGTGGCGACGGGAA	our laboratory (designed for Hypr and Neudoerfl)
TBEV probe sfRNA R	AGCGGGTGTTTTTCCGAGTCA	our laboratory (designed for Hypr and Neudoerfl)
HPRT1 F	TGACACTGGCAAAACAATGCA	Vandesompele *et al*., 2002
HPRT1 R	GGTCCTTTTCACCAGCAAGCT	Vandesompele *et al*., 2002

Amplification program for the qRT-PCR was performed under following conditions: 42°C for 10 minutes, initialisation at 95°C for 5 minutes, 40 cycles of denaturation at 95°C for 5s and annealing and elongation at 60°C for 30s.

All samples were analysed in technical triplicates using LightCycler® 480 (Roche Life Science) and melting curves were checked for every sample.

Obtained data were processed via relative quantification using the delta-delta c_t ($\Delta\Delta c_t$) method. C_T mean values for each sample triplicate were calculated together with standard deviations. The average c_t values of treated samples were normalised to a reference gene HPRT1 (Hypoxanthine Phosphoribosyltransferase 1). Eventually, relative quantification ($2^{\wedge}\Delta\Delta c_t$) was evaluated and the values were logaritmized.

4.5 Metabolic labelling of *de novo* synthesized proteins and rRNA

In this thesis, Click chemistry was used to incorporate labelled amino acid or NTP analogues into newly synthesised protein or RNA molecules, respectively. Bioconjugation is a highly efficient and convenient method as it is a great alternative to radioactive labelling and can be performed *in vitro* (Sletten and Bertozzi, 2009) and remarkably also *in vivo* (Agarwal *et al*., 2015).

Click chemistry is a class of bioorthogonal chemistry, which follows specific criteria. The chain of reactions of Click chemistry must be highly yielding, highly selective and occur at high speed (Baskin and Bertozzi, 2007). The copper-catalysed azide-alkyne cycloaddition reaction is a widely used Click reaction method. The azide and alkyne group form a very stable triazole ring as a linker (Huisgen, 1963) in an environment involving a monovalent copper ion as a catalyst (Rostovtsev *et al*., 2002). Either alkyne or azide group is ligated into the observed molecule and the other is labelled with a functional group (fluorophore, biotin) which can be later detected.

A simple schematic representation of a Click-reaction can be seen in Figure 7.

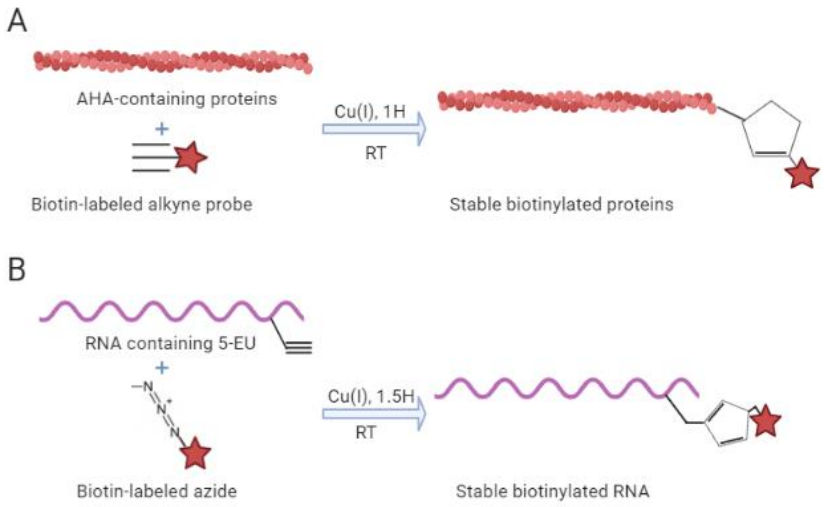

Figure 7: A schematic model of metabolic labelling principle (modified from CLICK-labelling of cellular metabolites, Jena Bioscience).

In our case, 4-Azido-L-homoalanine (AHA) or L-Homopropargylglycine (HPG) were used as an analogue of methionine to be incorporated into newly synthesised proteins in a methionine-deprived conditions. For metabolic labelling of RNA, 5-Ethynyl Uridine (5-EU) was used as a biorthogonal element in metabolic labelling method; proliferating cells used 5-EU analogue instead of uracil.

4.5.1 *Metabolic labelling of de novo synthesised proteins*

For the metabolic labelling of proteins, cells were seeded in RPMI medium in 12-well-plates. The experiment was conducted in separated biological triplicates. Fresh and filtered RPMI medium without methionine was prepared prior to the experiment, containing also 1% ATB, 1% L-alanyl-L-glutamine, 10% FBS and 0.21 mM L-cysteine.

Firstly, 0.75 ml of methionine-free RPMI medium was added to each well. The cells were starved for 2 hours at the same conditions (37°C and 5% CO_2). After the starving was completed, the starvation medium was removed. From this step, the experiment continued in the dark.

To each well, 750 µl of methionine-free RPMI medium with 50 µM AHA/HPG and 1× AlamarBlue™ Cell Viability Reagent (Thermo Fisher Scientific) was added. Two negative controls were set, MBP-transfected cells with AHA/HPG and cells without any transfection and no AHA/HPG. As a positive control, cells without transfection, but treated with AHA/HPG were prepared.

The reactions were incubated for 2 hours at 37°C and 5% CO_2. After the incubation, 150 µl of the medium was taken into 96-well-plate in technical duplicates and the cells were twice washed with PBS. The cells were then lysed in 250 µl of RIPA buffer (25 mM Tris-HCl pH 7.6, 150 mM NaCl, 1% NP-40, 0.1% SDS, 1% sodium deoxycholate) containing protease inhibitors (100× diluted, Halt™ Protease Inhibitor Single-Use Cocktail, Thermo Fisher Scientific) and the lysis was performed for 15 minutes on ice. The lysates were then transferred to 1.5 ml Eppendorf tubes and sonicated for 15 minutes. Subsequently, the samples were centrifuged at 14,000 g for 10 minutes at 4°C. The supernatant was transferred to a new 1.5 ml Eppendorf tube and the concentrations of proteins were determined using Pierce™ BCA Protein Assay Kit (Thermo Fisher Scientific Scientific) according to the manufacturer's protocol.

Briefly, 15 µl of each sample was transferred to a 96-well-plate. BCA working reagent was prepared by mixing reagent A and B in ratio 50:1 (A:B) and 200 µl of this mixture was added to each sample. Along with the samples, bovine serum albumin (BSA) standards were treated the same way. A simple diluent (milliQ water) was used as blank.

The samples were incubated at 37°C for 30 minutes and then analysed using Synergy H1 hybrid microplate reader (absorbance measured at wavelength of 562 nm, BioTek). After the measurement, the absorbance of the blank standard was subtracted from all samples and standards. Subsequently, a standard calibration curve from the absorbance and known concentration of the BSA standards was established. This curve was used to determine the concentrations of protein samples.

The samples were stored at -80°C until further use.

4.5.2 *Metabolic labelling of de novo synthesised rRNA*

For the metabolic labelling of rRNA, cells were seeded and transfected in DMEM medium in 6-well-plates. The experiment was conducted in separate biological triplicates, After the PBS washing steps following transfection, 1 ml of fresh DMEM medium containing 1 mM 5-EU and 1× AlamarBlue™ Cell Viability Reagent was added to the wells. Similar to the protein labelling experiments, two negative controls were set – MBP-transfected cells treated with 5-EU, and cells lacking transfection and 5-EU. Healthy proliferating cells treated with 5-EU were used as positive control. The reactions were incubated for 4 hours at 37°C and 5% CO_2.

Following the metabolic labelling, 200 µl of the volume from the wells was transferred into 96-well-plate in technical duplicates and the wells were then washed twice with PBS. The cells were lysed using RNA Blue reagent according to the manufacturer's protocol (see 4.4.1). The yielded RNAs were stored at -80°C.

4.5.3 *Measuring viability of cells for sample standardisation*

For metabolic labelling analyses, normalisation to cell numbers was performed using AlamarBlue™ Cell Viability Reagent. Viability measurement of the cells is equivalent to the cell number (Selinger *et al*., 2019).

As mentioned in the previous chapter, 150 µl or 200 µl from each well (depending on the size of the wells) was transferred into 96-well-plate in technical duplicates. For the fluorescence measurement, the technical duplicates were then analysed using Synergy H1 hybrid microplate reader (λ_{ex} = 550 nm; λ_{em} = 590 nm, BioTek). RPMI-methionine free medium with 50 µm AHA/HPG or DMEM medium with 1 mM 5-EU without cells, both with 1× AlamarBlue™ Cell Viability Reagent, was used as blank.

Average fluorescence values for sfRNA-transfected samples were normalized to the respective mock control cells. The viability factor (f) was used as a normalization factor for the evaluation of RNA/protein loading input based on the mock control input (Selinger *et al*., 2019).

$$f = \frac{viability_{sample}\,[a.u.]}{viability_{control}\,[a.u.]} \qquad V_{sample} = \frac{V_{control}\,[\mu l]}{f}$$

4.6 Click-on-membrane assay of *de novo* synthesized proteins

4.6.1 *SDS-PAGE*

Firstly, proteins were separated according to size using polyacrylamide gel electrophoresis. The separation gel contained 12% acrylamide (Rotiphorese® Gel 30 mixture of acrylamide and bis-acrylamide 37.54:1, Roth); 0.1% APS; 0.375 M Tris-base pH 8.8; 0.1% SDS and 0.004% TEMED (N,N,N',N'-Tetramethylethylendiamin). The stacking gel contained 5% acrylamide; 0.25 M Tris-base pH 6.8; 0.1% SDS; 0.1% APS and 0.01% TEMED.

The volume of each sample loaded on gel was normalized to the cell number measured after the metabolic labelling procedure, where 5 µg of un-transfected AHA/HPG-labelled cells was counted as 100% (see 4.5.3). All samples were mixed with 5× concentrated reducing buffer

without DTT (0.2% bromothymol blue, 40% glycerol, 8% SDS, 0.2 M Tris-HCl) in 1:4 ratio (sample:buffer; v/v) and incubated for 10 minutes at RT. Electrophoresis buffer (25 mM Tris-base, 0.192 M glycine, 0.1% SDS) was added in an assembled electrophoretic apparatus (Mini-PROTEAN® Tetra Cell, Bio-Rad), and the samples as well as protein marker (Prestained Protein Marker VI 10-245 kDa, Applichem) were loaded onto the gel. The electrophoretic separation ran for 1.5 hours at 120 V. After the separation, gels were used for western blotting and eventually stained with PageBlue™ Protein Staining Solution (Thermo Fisher Scientific) overnight. The stained gels were analysed using Syngene™ Gbox Chemi XX6.

4.6.2 *Western blotting*

Electrophoretically separated proteins were transferred onto a PVDF membrane (Amersham).

Briefly, the membrane was firstly activated in methanol for 5 minutes, then incubated in dH_2O and blotting buffer (25 mM Tris-HCl, 192 mM glycine, 20% methanol). Gels along with blotting papers were incubated in blotting buffer as well. Blotting sandwich was assembled in blotting apparatus (Trans-Blot® Turbo™ Transfer System, Bio-Rad) and the transfer took 30 minutes at 25 V and 1A as maximum current.

4.6.3 *Click-on-membrane assay*

The Click-on-membrane detection method was performed following methodology by Kočová *et al*. (in preparation).

Following the blotting procedure, the membranes were washed in dH_2O for 1 minute and then equilibrated in 0.1 M potassium phosphate buffer (pH 7.0). For each membrane, a reaction mixture was prepared following Presolski *et al*. (2011). The mixture contained 400 µl sodium ascorbate (0.1 M), 80 µl THPTA (Tris(3-hydroxypropyltriazolyl-methyl)amine, 50 mM), 40 µl $CuSO_4$ (20 mM), 16 µl biotin-alkyne/picolyl biotin azide (5 mM) and the volume was adjusted to 8 ml with potassium phosphate buffer (0.1 M).

The mixture was then added onto the membrane and incubated for 1 hour at RT in the dark.

After the Click-on-membrane reaction was finished, the membrane was twice washed in PBS-T (PBS, 0,05% Tween) for 5 minutes and then incubated in a blocking solution (5% non-fat

milk in PBS-T) for 1 hour. The membrane was then directly incubated with primary antibody in blocking solution (Goat Anti-Biotin, 1:1000, Vector Laboratories) overnight at 4°C on shaker. Subsequently, the membrane was thrice washed in PBS-T for 5 minutes and then incubated in secondary antibody (Peroxidase labelled Anti-Goat IgG, 1:1000, Vector Laboratories) for 1 hour at RT. Finally, the membrane was thrice washed in PBS for 5 minutes and the signal was developed by using WesternBright Quantum HRP substrate (Advansta) according to manufacturer's protocol and analysed using Syngene™ Gbox Chemi XX6.

4.7 Click-on-membrane assay of *de novo* synthesized rRNA

4.7.1 *Agarose electrophoresis*

The yielded total RNAs were separated according to their size using denaturing agarose gel electrophoresis. 1.2% agarose MOPS-buffered denaturing gel (with 6.7% formaldehyde and GelRed® Nucleic Acid Gel Stain, Millipore) was used for the fractionation. All buffers were diluted in DEPC-treated H_2O and all used glassware and plasticware was sterile.

The volume of each sample loaded on gel was normalized to the cell number measured after the metabolic labelling procedure, where 5 µg of un-transfected 5-EU-labelled cells was counted as 100% (see 4.5.3). All samples were mixed with 2× concentrated reducing buffer (62.5% formamide, 0.35%formaldehyde, 0.2625% MOPS) and incubated for 10 minutes at 75°C. The electrophoretic apparatus was assembled and electrophoretic buffer (1× MOPS) was added. Pre-electrophoresis was performed with empty gel for 5-10 minutes in order to remove residual ions from the wells. The samples were loaded on the gel as well as RNA marker (RiboRuler High Range RNA Ladder, Thermo Fisher Scientific) and the electrophoretic separation ran for approximately 2 hours at 90 V. The GelRed signal of the gel was subsequently viewed using Syngene™ Gbox Chemi XX6 and Fiji software.

4.7.2 *Northern blotting*

The gel was washed in DEPC-treated H_2O for 30 minutes followed by incubation in 50 mM NaOH for 15 minutes. Subsequently, the gel was equilibrated in 20× SSC (3 M NaCl, 0.3 M sodium citrate dihydrate, pH 7.2) for 30 minutes.

The separated RNAs were transferred from the gel onto a PVDF membrane (Amersham). Firstly, the membrane was incubated for 5 minutes in methanol, washed in

DEPC-treated H_2O for 2 minutes and then equilibrated in 5× SSC for 5 minutes. Blotting papers were also wetted with 20× SSC. The blotting sandwich was assembled (shown in Figure 8) and the capillary transfer ran overnight at RT.

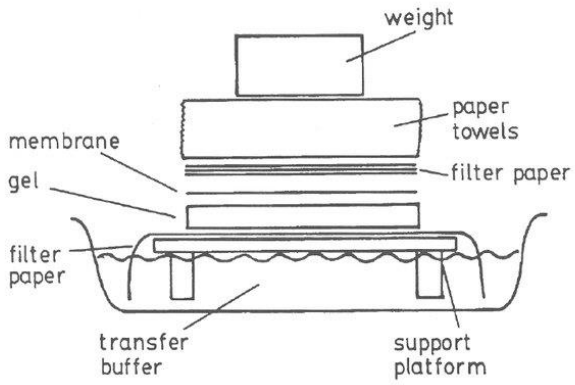

Figure 8: A schematic model of Northern blotting sandwich assembly (adapted from Karcher, 1991).

The following day, the sandwich was disassembled and the membrane was washed in 5× SSC for 5 minutes and air-dried. Finally, the membrane was UV cross-linked (1200×10^2 μJ/cm^2) using UVP Crosslinker Legacy Model (Analytik Jena).

4.7.3 *Click-on-membrane assay*

The Click-on-membrane detection method was performed according to Kočová *et al*. (in preparation). The UV cross-linked membrane was equilibrated in 0.1 M potassium phosphate buffer and then incubated in Click-on-membrane solution (see 4.6.3) with biotin picolyl azide for 1.5 hours in the dark. Subsequently, the membrane was washed in PBS for 10 minutes and then incubated in a blocking solution (3% bovine serum albumin – BSA, in PBS) for 1 hour at RT.

The incubation in primary and secondary antibodies (in 3% BSA) as well as developing of the signal is identical to the Click-on-membrane assay of proteins (see 4.6.3.).

4.8 Fluorescence *in situ* hybridization

4.8.1 *Transfection and infection of DAOY HTB-186 cells*

DAOY HTB-186 cell line was seeded into chambered slides (Thermo Fisher Scientific) in DMEM medium at a density of 1.25×10^4 cells per well and grown for 24 hours. The following day, the cells were either transfected by *in vitro* transcribed sfRNA or infected by TBEV Hypr or Neudoerfl strains. Each transfection and infection was performed in technical triplicates.

4.8.1.1 Transfection of chambered cells

Lipofectamine® RNAiMAX Transfection Reagent (Thermo Fisher Scientific) and Polyjet™ *In vitro* DNA Transfection Reagent were used for the transfection with 100 ng of sfRNA of DENV, ZIKV, TBEV (Hypr and Neudoerfl strain) per well according to the manufacturer's protocol. For negative control, 100 ng per well of MBP was used.

The cells were transfected for 24 hours and fixed either with 4% paraformaldehyde, methanol, acetone or DSP (dithiobis(succinimidyl propionate)), Thermo Fisher Scientific) according to Table III.

Briefly, DSP is a water-insoluble cross-linker which is thiol-cleavable and primary amine-reactive. Additionally, it is useful as an intracellular cross-linker because it is lipophilic and easily crosses cell membrane. N-hydroxysuccinimide esters contained in DSP structure react at pH 7-9 with primary amines of target proteins to form stable amide bonds (Thermo Fisher Scientific User Guide). The cells were introduced to DSP at final concentration of 2 mM (in PBS) for 30 minutes at RT and the reaction was stopped by adding Tris-HCl (pH 7.5) at final concentration of 20 mM.

The cells were eventually thoroughly washed with PBS and used for hybridization.

Table III: Fixation reagents, times and temperatures used for the fixation of DAOY HTB-186 cells following transfection or infection.

Fixation reagent	**Fixation time**	**Temperature**
paraformaldehyde (ROTI® Histofix 4%, Roth)	15	RT
methanol	30	-20°C
acetone	30	-20°C
DSP	30	RT

4.8.1.2 Infection of chambered cells

For the infection of DAOY cells, two representatives of the West-European TBEV subtype were used. TBEV Hypr (GenBank accession no. U39292, 2.7×10^8 pfu/ml) and TBEV Neudoerfl (GenBank accession no. U27495, 4.04×10^8 pfu/ml). The viruses were added to cells one day post seeding at an MOI of 5. Brain suspension from uninfected suckling mice was used as a negative control. Infection was performed under biosafety level 2 conditions.

The cells were incubated with the virus for 24 hours and fixed with 4 alternative fixation reagents (see Table III). The cells were eventually thoroughly washed with PBS and used for hybridization.

4.8.2 *DNA probe preparation by PCR*

For fluorescence *in situ* hybridization (FISH), DNA probes complementary to sfRNAs of TBEV (Hypr and Neudoerfl strain) were prepared by PCR using Q5® Hot Start High-Fidelity DNA Polymerase (NEB) according to the manufacturer's instructions. The DNA probe of 298 bp complementary to the 3'UTR region (sfRNA) of both strains is practically identical and varies only in 4 nucleotide substitutions which can be seen in Table IV. Hypr sfRNA probe (nucleotides 10,538 to 10,836) and Neudoerfl sfRNA probe (nucleotides 10,844 to 11,141) were prepared using the exact same primers whose primer sequences can be found in Table II (see 4.4.2). As a template for the PCR, pDEST40-TBEV Hypr/Neudoerfl 3'UTR and pC-wt plasmids were used.

Table IV: Difference in base substitutions in the 3'UTR region (sfRNA) of TBEV Hypr strain and TBEV Neudoerfl strain.

base substitution	Hypr	Neudoerfl
10,593	C	T
10,642	A	G
10,659	T	C
10,791	A	G

Additionally, a DNA probe for the flaviviral C protein was also prepared. The probe of 288 bp (nucleotides 133 to 421) is also highly identical for both TBEV strains used for hybridization, differing in 6 nucleotide substitutions which can be seen in Table V.

Table V: Variations of base substitutions in the C protein of TBEV Hypr strain and TBEV Neudoerfl strain.

base substitution	Hypr	Neudoerfl
243	C	T
285	T	C
345	C	A
375	A	C
408	C	T
411	A	G

The PCR reaction mixture was prepared according to Table VI.

Table VI: Reaction setup for PCR using Q5® Hot Start High-Fidelity DNA Polymerase (NEB) for a 50 µl reaction.

Reagent	Volume (µl)
5× G5 Reaction Buffer	10
2 mM dNTPs	5
10 µM F primer	1.5
10 µM R primer	10
5× Q5 High GC Enhancer	0.5
≈100 ng of plasmid	x
Q5 Hot Start DNA Polymerase	0,5
nuclease-free H_2O	to 50 µl

Amplification program using T100™ Thermal Cycler (Bio-Rad) was performed under following conditions: initial denaturation at 98°C for 30s, 35 cycles of denaturation at 95°C for 10s and annealing and elongation at 60°C for 10s and 72°C for 20s followed by final extension at 72°C for 2 minutes. The yielded DNA was precipitated, stored at -20°C or directly used for hybridization.

4.8.3 *DNA precipitation*

DNA obtained from Q5 PCR was precipitated using Phenol/Chloroform/Isoamyl DNA isolation protocol. Briefly, the equivalent volume of ROTI® Phenol/Chloroform/Isoamyl alcohol (25:24:1; v/v; Roth) was added to the PCR reaction, thoroughly vortexed and incubated for 5 minutes at RT. The mixture was subsequently centrifuged at 13,000 × g for 10 minutes. The aqueous phase was transferred to a new 1.5 ml Eppendorf tube and pre-chilled 96% ethanol was added in 3:1 ratio (ethanol:sample, v/v) together with 3 M sodium acetate (pH 5.5) in 1:9 ratio (sodium acetate:sample, v/v). The mixture was then incubated for 30 minutes at -20°C and centrifuged at 16,000 × g for 30 minutes at 4°C.

The supernatant was discarded and the DNA pellet was washed with pre-chilled 75% ethanol. After the final centrifugation at 16,000 × g for 10 minutes at 4°C, the supernatant was removed and the DNA was air-dried for 5-10 minutes. The precipitate was eventually

dissolved in milli-Q ultrapure H_2O. The concentration of the DNA was measured using the NanoPhotometer®.

The integrity of the yielded DNA probe was checked using agarose gel electrophoresis on a 1% agarose gel. Both DNA probe sample and marker (100 bp DNA Ladder Plus, Thermo Fisher Scientific) were mixed with 6× DNA-loading buffer with GelRed® Nucleic Acid Gel Stain. The electrophoretic buffer (1× TAE) was filled into the apparatus and the samples were loaded on the gel. The electrophoretic separation ran for 1 hour at 100 V and the gel was subsequently viewed using Syngene™ Gbox Chemi XX6.

4.8.4 *DNA probe labelling*

For our hybridization, direct and indirect florescence experiments were performed. In the case of indirect labels, digoxigenin-11-dUTP (DIG, Jena Bioscience) and biotin-11-dUTP (Biotin, Jena Bioscience) labelling systems were used. Secondly, fluorescein-12-dUTP (FITC, Fermentas) was used for direct fluorescence.

4.8.4.1 Nick translation

Nick translation is an efficient labelling technique, which results in the replacement of some nucleotides in a DNA sequence with labelled analogues. Briefly, the DNase treatment leads to the production of single-stranded fragments (nicks) in the dsDNA molecule. Labelled nucleotides are subsequently incorporated by DNA Polymerase I during the nick replacement (Rigby *et al.*, 1977).

Nick translation reaction was prepared according to Table VII. 10× Nick Translation buffer (0.5 M Tris-HCl pH 7.5, 50 mM $MgCl_2$, 0.05% BSA and dH_2O) and 0.1 M β-Mercaptoethanol were prepared fresh prior to the reaction.

Table VII: Nick translation reaction mixture.

Reagent	Volume (µl)
10× Nick Translation Buffer	2
0.1 M β-Mercaptoethanol	2
dNTPs for labelling	2
1 mM labelled dUTPs	0,4
DNA Polymerase I	2
100× DNase	0,5
≈1 µg of DNA probe	x
nuclease-free H_2O	to 20 µl

The mixture was then incubated for 2 hours at 15°C. The inactivation of the enzymes was performed by incubation of the reaction at 70°C for 10 minutes. The yielded labelled DNA probes were directly used for hybridization.

4.8.4.2 DecaLabel™ DNA Labelling (random decamers)

Firstly, approximately 1 µg of DNA probe was mixed with 10 µl of Decanucleotide mix in 5× Reaction Buffer and filled to 40 µl with nuclease-free H_2O. This mixture was briefly vortexed, spun down in a microcentrifuge for 5s, incubated at 100°C for 5-10 minutes and cooled on ice. Subsequently, 3 µl of Mix T (mixture of 5mM dATP, dCTP, dGTP and 1mM dTTP), 1 µl of labelled dUTPs (DIG or FITC) and 1 µl of Klenow fragment was added. The mixture was vortexed, spun down and incubated at 37°C for 1 hour. The reaction was eventually terminated by addition of 1 µl of 0.5 M EDTA (pH 8.0).

In the case of Biotin Labelling Kit, approximately 1 µg of DNA probe was mixed with 10 µl of Decanucleotide in 5× Reaction Buffer and filled to 44 µl with nuclease-free H_2O. The mixed components were then vortexed, spun down, incubated at 100°C for 5-10 minutes and cooled on ice. Subsequently, 5 µl of Biotin Labelling Mix and 1 µl of Klenow fragment was added, the mixture was shaken, centrifuged and incubated at 37°C for 1 hour. The reaction was stopped by addition of 1 µl of 0.5 M EDTA (pH 8.0).

The labelled DNA probes were immediately used for hybridization.

4.8.5 *Fluorescence in situ hybridization*

All solutions used for fluorescence *in situ* hybridization were prepared fresh and filtered (PES filters, 0.2 µm pores).

Cells fixed with paraformaldehyde and DSP were permeabilized using 0.1% Triton X-100 in PBS for 15 minutes followed by two PBS washes for 5 minutes each. The cells were then treated with 50 mM NH_4Cl in PBS as a quenching solution for 10 minutes. Each well was then washed twice with PBS again.

Additionally, endogenous biotin in cells was subsequently blocked using Avidin/Biotin Blocking kit (Vector Laboratories) in 3% BSA according to the manufacturer's protocol. The cells were thoroughly washed with PBS and were directly used for hybridization.

4.8.5.1 Direct fluorescence in situ hybridization

Each well was covered with 100 µl of hybridization buffer which contained 50 µl of formamide, 20 µl of 50% dextran sulfate sodium salt (w/v), 10 µl of 20× SSC, 1 µg of denatured FITC-labelled probe, DEPC-treated H_2O adjusted to the final volume. The slides were subsequently heated at 70°C for 5 minutes and hybridized in an air-tight box with a 2× SSC-wetted tissue at 42°C overnight.

The following day, the hybridization buffer was removed and the wells were washed in 2× SSC for 10-15 minutes at 42°C. After washing, chambers were removed from the slides and hybridized cells on the slides were immediately mounted with Roti® -Mount Fluor-Care with DAPI (Roth) without drying and covered with cover glass.

Finished slides were stored at 4°C and analysed using confocal microscope (FluoView FV10i, Olympus).

4.8.5.2 Indirect fluorescence in situ hybridization

Each well was covered with 100 µl of hybridization buffer which contained 50 µl of formamide, 20 µl of 50% dextran sulfate sodium salt (w/v), 10 µl of 20× SSC, 1 µg of denatured DIG/Biotin labelled probe, DEPC-treated H_2O adjusted to the final volume. The slides were subsequently heated at 70°C for 5 minutes and hybridized in an air-tight box with a 2× SSC-wetted tissue at 42°C overnight.

Following the overnight hybridization, the slides were washed once in 2× SSC for 15 minutes at 42°C. Subsequently, the slides were incubated in a blocking solution of 3% BSA in PBS for 1 hour at RT. After blocking, 100 µl of 1% BSA and Anti-DIG DyLight® 488 (1:200, Vector Laboratories) or Streptavidin DyLight® 549 (1:200, Vector Laboratories) was added to each well and incubated for 1.5 hours at RT.

Eventually, the wells were 5× washed with PBS, the chambers were removed from the slides and the cells were air-dried for 5-10 minutes. Then they were treated in the exact way as in the previous chapter (4.8.5.1.), stored at 4°C and used for analysis (FluoView FV10i, Olympus).

5. Results

5.1 Optimisation of cell transfection with *in vitro* transcribed sfRNA

Very little is known about the function of sfRNA from TBFs, since majority of sfRNA studies has been focused primarily on MBFs such as DENV, WNV, and ZIKV. Therefore, in this thesis, TBEV Hypr and Neudoerfl strains have been chosen for the sfRNA functional analyses, where ZIKV and DENV sfRNAs served as a comparison from the group of MBFs. For this purpose, pDEST40 constructs carrying 3'UTRs from four flaviviruses (DENV-2, ZIKV PE243, TBEV strain Hypr and Neudoerfl) were utilized for the *in vitro* transcription and subsequent transfection.

The first part of this thesis was focused on determination of the dynamics of sfRNA levels in transfected DAOY HTB-186 cells. Two transfection time intervals were chosen for the relative real-time PCR quantification in order to determine whether the accumulation of sfRNA in transfected cells is higher at 24 or 48 hours p.t. (Figure 9).

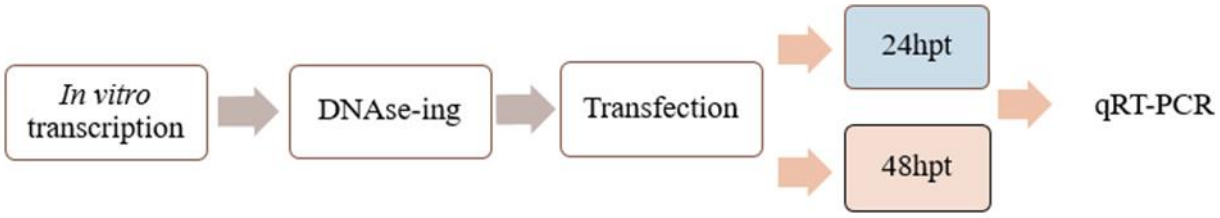

Figure 9: Optimisation of transfection in subsequent steps.

The total RNA from transfected cells was diluted according to the viability factor and the levels of the respective sfRNA were analysed by qRT-PCR. Relative quantification of each sample was calculated using $_{\Delta\Delta}c_{t.}$ The graphic representation of the $\log_{10}$ fold-change of sfRNA levels can be seen in Figure 10.

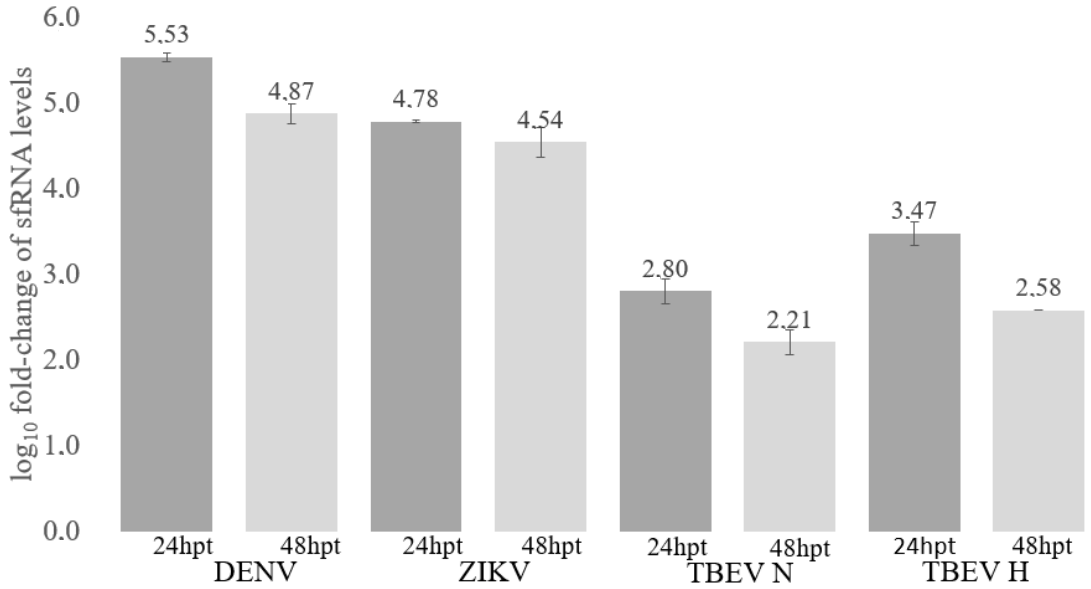

Figure 10: The $\log_{10}$ fold-change of sfRNA levels of selected flaviviruses (DENV, ZIKV, TBEV Neudoerfl strain (N) and TBEV Hypr strain (H) 24 and 48 hours p.t.

The results show that the quantity of sfRNA in transfected cells is slightly higher in the first 24 hours after the transfection. This indication led us to further use the 24-hour transfection interval in all following experiments.

5.2 Determination of the effect of sfRNA on *de novo* synthesized proteins of the host cells

The ability of sfRNA to inhibit translation of several genes has been observed in DENV by Bidet *et al*., 2014. Recently, TBEV was also observed to induce host translational shut-off during ongoing infection in DAOY cells (Selinger *et al*., 2019), however, the mechanism has not yet been determined. Since sfRNA in MBFs was observed to strongly modulate host environment, the next aim of this thesis, after the confirmation of the accumulation of sfRNA species in transfected cells, was to determine whether it plays a role in biasing the host synthesis of proteins.

The schema of the experiment is shown in Figure 11.

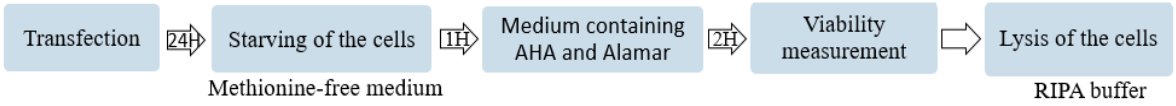

Figure 11: The timeline of metabolic labelling of newly synthesised proteins assay using AHA/HPG analogue of methionine.

The metabolic labelling assay was performed in biological triplicates and initially, the methionine analogue used in the protocol was AHA. Unfortunately, the relative AHA signal led to high speckled background and the signal was overall not conclusive in several attempts of Click-on-membrane assay, so the labelling method was switched to HPG analogue.

The methionine-starved cells were forced to incorporate HPG into newly synthesised proteins due to the abundance of the methionine analogue. Therefore, the newly synthesised proteins were possible to detect using Click-on-membrane assay (Kočová *et al*., in preparation). The relative HPG signal of newly synthesised proteins from sfRNA transfected cells of selected flaviviruses (DENV, ZIKV, TBEV strain Neudoerfl and Hypr) was then compared to the relative HPG signal of MBP-transfected cells which were taken as a negative control (Figure 13). A representative image of a Click-on-membrane assay is shown in Figure 12.

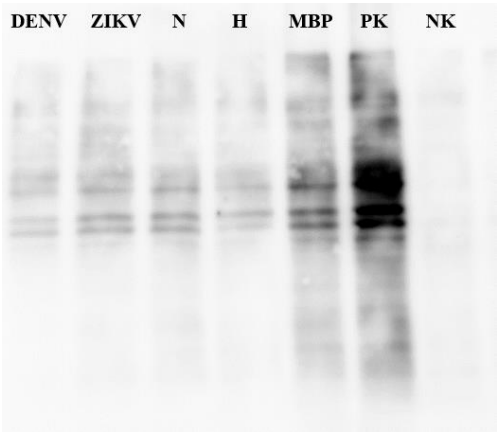

Figure 12: Click-on-membrane assay of HPG labelled *de novo* synthesised proteins. DENV – dengue virus, ZIKV – zika virus, N – TBEV Neudoerfl strain, H – TBEV Hypr strain, MBP – maltose-binding protein, PK – positive control, NK – negative control. A representative image from three independent biological replicates is shown.

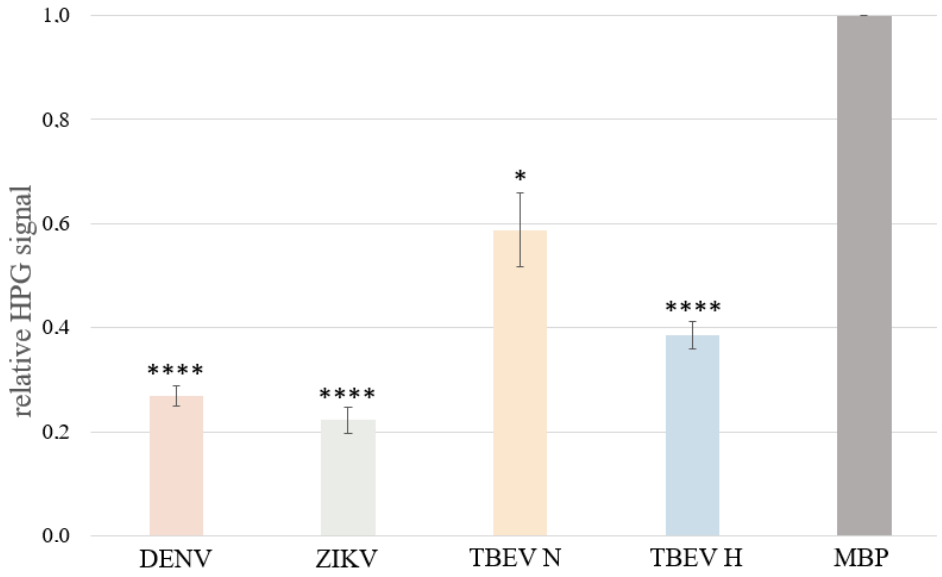

Figure 13: The relative HPG signal of *de novo* synthesised proteins from DAOY cells transfected with selected sfRNA species from DENV, ZIKV, TBEV strain Neudoerfl (N) and TBEV strain Hypr (H). MBP-transfected cells served as negative control. The data represent mean values from three independent biological replicates. Significant difference from control was calculated by unpaired Student's t-test (α=0.05, * P < 0.05, ** P <0.01, *** P <0.001, **** P < 0.0001).

The graphic representation of the relative HPG signal indicated that the production of *de novo* synthesised proteins is decreased in cells treated with sfRNAs from all flaviviruses tested. The most significant difference can be observed from the transfection of DENV (Student's t-test, α=0.05, p=0.82E-6) and ZIKV (Student's t-test, α=0.05, p=0.17E-5) sfRNA species. However, in the case of TBEV, Hypr strain (Student's t-test, α=0.05, p=0.014) shows a more considerable decrease of host protein synthesis than Neudoerfl strain (Student's t-test, α=0.05, p=0.51E-5).

5.3 Determination of the effect of sfRNA on *de novo* synthesized rRNA of the host cells

Additionally, not only translational shut-off was observed in TBEV infected cells. TBEV also interferes with host *de novo* production of 45-47S pre-rRNA transcripts and the transcription levels of 18S and 28S rRNA in infected cells is decreased up to 50% (Hypr strain), but the mechanism of the downregulation remains unknown (Selinger *et al*., 2019).

Consequently, the possible function of sfRNA to regulate the *de novo* synthesis of host rRNA was examined. DAOY HTB-186 cells transfected with *in vitro* transcribed sfRNA were

incubated with 5-EU in a high concentration (1mM) so the cells were forced to incorporate the uracil analogue during RNA synthesis (Figure 14.).

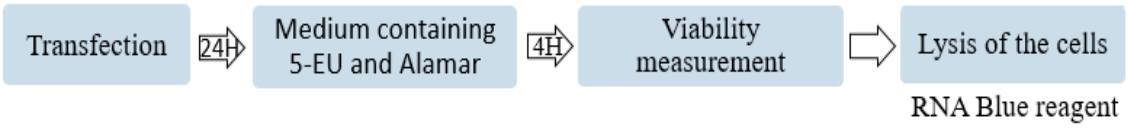

Figure 14: Metabolic labelling of newly synthesised rRNA protocol shown in a timeline.

The labelled rRNA was detected using the Click-on-membrane assay (Kočová *et al.*, in preparation) and the relative 5-EU signal of newly synthesised rRNA from sfRNA transfected cells of selected flaviviruses (DENV, ZIKV, TBEV Neudoerfl and Hypr strains) was then compared to the relative signal of MBP-transfected cells (Figure 16). A representative image of a Click-on-membrane assay is shown in Figure 15.

Figure 15: Click-on-membrane assay of 5-EU labelled *de novo* synthesised rRNA. DENV – dengue virus, ZIKV – zika virus, N – TBEV Neudoerfl strain, H – TBEV Hypr strain, MBP – maltose-binding protein, PK – positive control, NK – negative control. A representative image from three independent biological replicates is visualized.

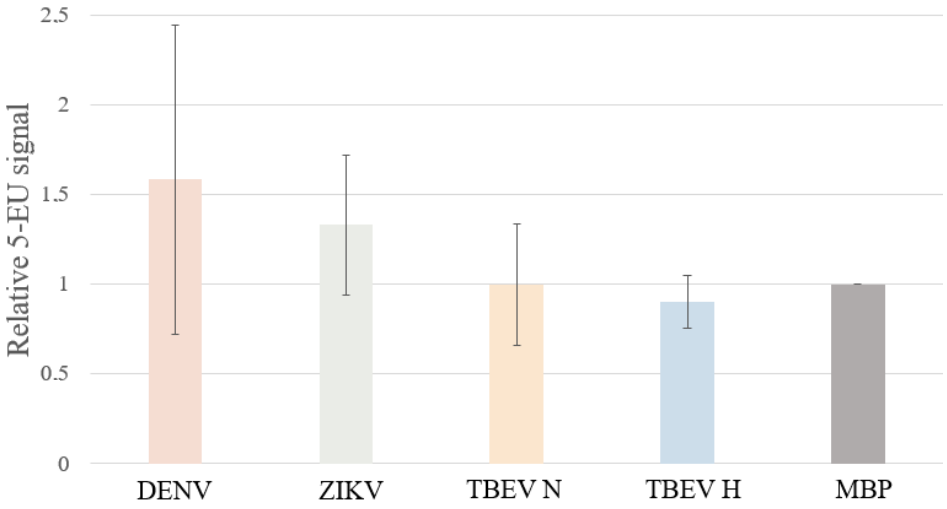

Figure 16: The relative 5-EU signal of *de novo* synthesised rRNA from DAOY cells transfected with selected sfRNA species from DENV, ZIKV, TBEV strain Neudoerfl (N) and TBEV strain Hypr (H). MBP-transfected cells served as negative control. The data represent mean values from three independent biological replicates. Significant difference from control was calculated by unpaired Student's t-test (α=0.05, * P < 0.05, ** P <0.01, *** P <0.001, **** P < 0.0001).

The relative 5-EU signal levels of sfRNA transfected cells in comparison to negative control were not significantly decreased for any flavivirus tested – DENV (Student's t-test, α=0.05, p=0.39), ZIKV (Student's t-test, α=0.05, p=0.3), TBEV Hypr strain (Student's t-test, α=0.05, p=0.99) and TBEV Neudoerfl strain (Student's t-test, α=0.05, p=0.39). Therefore, sfRNA probably does not play a role in reducing host rRNA synthesis.

5.4 Localisation of sfRNA in transfected and infected cells using fluorescence *in situ* hybridization

Since sfRNA affects the infected cells in several different aspects, the final step of this thesis was to localise sfRNA in transfected and infected cells to explore its functions in more detail. The localisation of sfRNA would be a great key to be able to precisely pinpoint its affect to certain cell compartments but also evaluate co-localisation sites with particular cell or viral factors. For the localisation itself, FISH was chosen as it is a powerful tool to visualize target RNA in cells and was previously demonstrated to work with sfRNA species in WNV-infected cells (Pijlman *et al*., 2008) and to study TBEV-infected cells (Hirano *et al*., 2017).

Several different aspects were tested for the optimisation of preparing slides for FISH. Firstly, two transfection reagents (Polyjet^{TM} *In vitro* DNA Transfection Reagent and

Lipofectamine® RNAiMAX Transfection Reagent) were considered for the transfection of DAOY HTB-186 cells.

Secondly, the preparation of DNA probes was also optimised with several alternatives. In order to determine the optimal labelling protocol for FISH, two labelling methods (random decamers and nick translation) were performed in combination with direct (FITC-dUTP) and indirect (Biotin-dUTP, DIG-dUTP) detection.

The experiments were performed with DAOY HTB-186 cells, which were either infected with TBEV strain Hypr/Neudoerfl (5 MOI, 24 hours post infection) or transfected with Hypr/Neudoerfl sfRNAs (1.25×10^4 cells per well, 24 hours p.t.).

The highly conserved region of TBEV 3'UTR (nucleotides 10,538 to 10,836 for Hypr and nucleotides 10,844 to 11,141 for Neudoerfl) was used for DNA probe preparation. Selected probe sequence is 298 bp long and almost identical for both strains (varying only in 4 nucleotide substitutions, see 4.8.2). In order to distinguish the sfRNA and 3'UTR region of viral gRNA in case of TBEV-infected cells, additional DNA probe targeting C protein gene was also prepared.

The DNA templates used for the probe preparation were first checked for their integrity by agarose gel electrophoresis on a 1% agarose gel prior to the labelling protocol (Figure 17.).

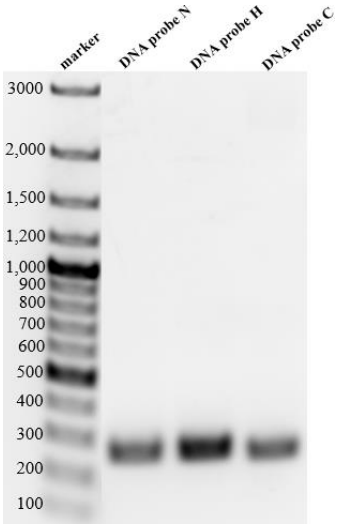

Figure 17: DNA probes prepared by PCR electrophoretically separated on a 1% agarose gel stained with GelRed® Nucleic Acid Gel Stain. Marker (100 bp DNA Ladder Plus, Thermo Fisher Scientific), DNA probe for sfRNA of Hypr (H) and Neudoerfl (N) strain (298 bp) and DNA probe C (for C protein gene, 288 bp) viewed using Syngene™ Gbox Chemi XX6.

For all FISH slides, MBP-transfected or mock-infected cells were used as a negative control for signal specificity comparison. Prepared mounted slides were analysed using FluoView FV10i confocal microscope (Olympus) with equal conditions for sensitivity and laser intensity for all sfRNA species. The final pictures were generated using FV10-ASW 4.2 Viewer (Olympus).

Data summarized in Figures 18, 19 and 20 are representatives of two independent experiments.

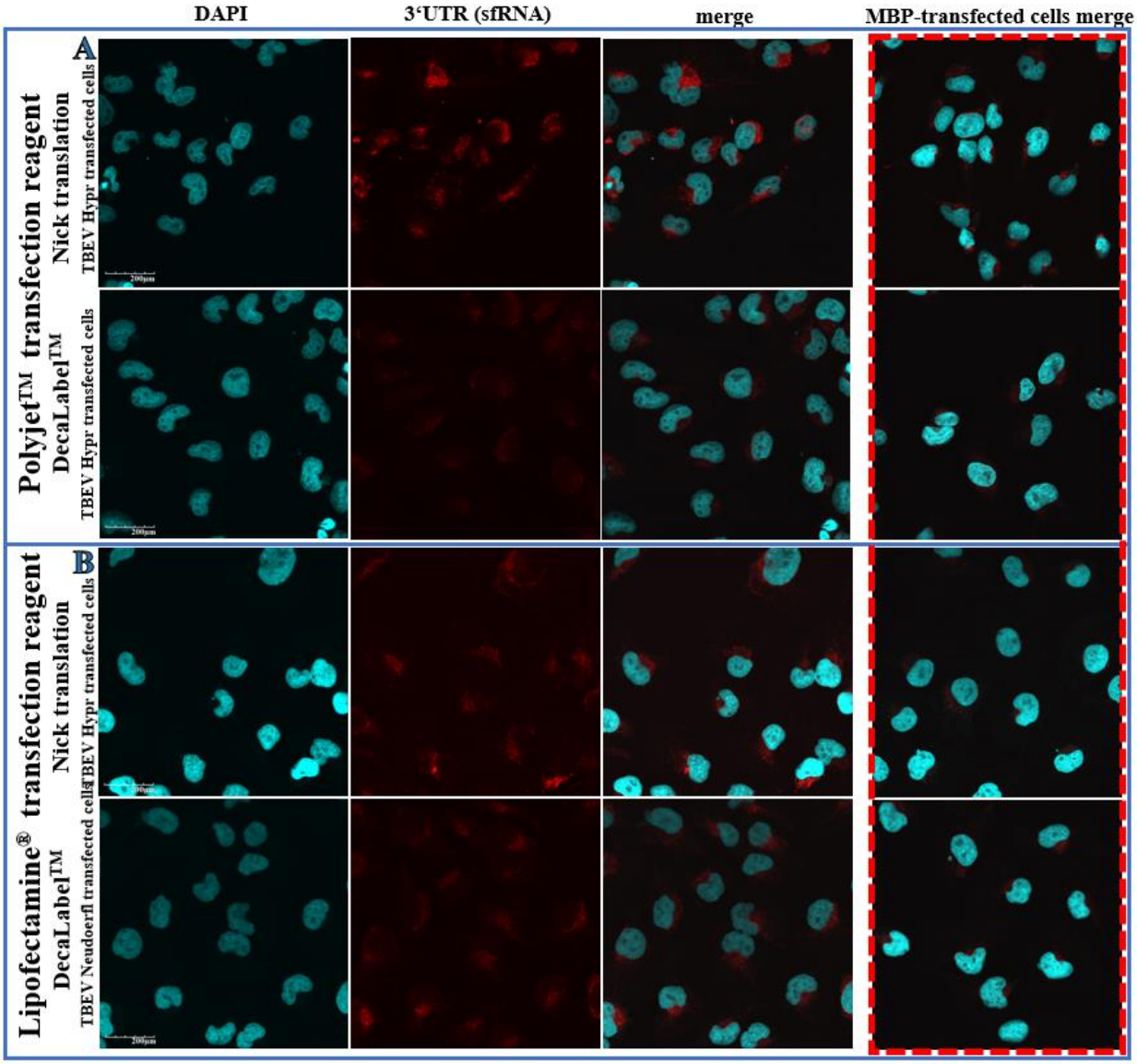

Figure 18: Indirect (Biotin-Streptavidin DyLight® 549) FISH of DAOY HTB-186 cells transfected with *in vitro* transcribed sfRNA of TBEV Hypr strain (H). **A)** DAOY cells were transfected using Polyjet™ *In vitro* DNA Transfection Reagent. Biotinylated DNA probe complementary to the 3'UTR (sfRNA) of TBEV H was prepared by nick translation or DecaLabel™ DNA Labelling kit. The hybridized biotinylated probe was detected using Streptavidin DyLight® 549. **B)** DAOY cells were transfected using Lipofectamine® RNAiMAX Transfection Reagent. Biotinylated DNA probe complementary to the 3'UTR (sfRNA) of TBEV H was prepared by nick translation or DecaLabel™ DNA Labelling kit and the signal was further visualised using Streptavidin DyLight® 549. Nuclei were stained with DAPI. Scale bar represents 200 µm.

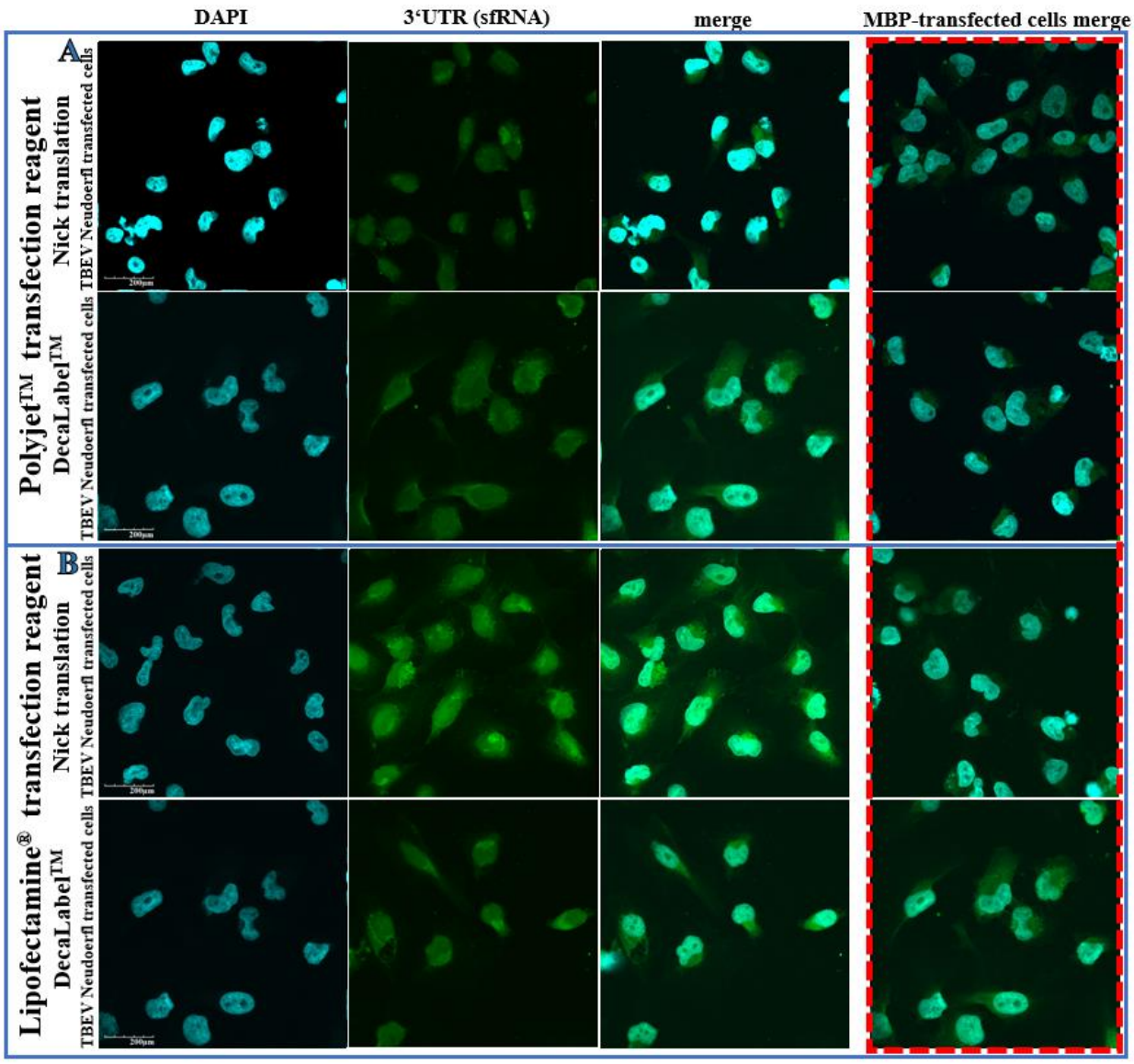

Figure 19: Indirect (DIG-Anti-DIG DyLight® 488) FISH of DAOY HTB-186 cells transfected with *in vitro* transcribed sfRNA of TBEV Neudoerfl strain (N). **A)** DAOY cells were transfected using Polyjet™ *In vitro* DNA Transfection Reagent. DNA probe (complementary to the 3'UTR (sfRNA) of TBEV (N) conjugated with DIG was prepared by nick translation or DecaLabel™ DNA Labelling kit. The hybridized DIG-probe was detected using Anti-DIG DyLight® 488. **B)** DAOY cells were transfected using Lipofectamine® RNAiMAX Transfection Reagent. DNA probe (complementary to the 3'UTR (sfRNA) of TBEV (N) conjugated with DIG was prepared by nick translation or DecaLabel™ DNA Labelling kit and the signal was subsequently visualised using Anti-DIG DyLight® 488. Nuclei were stained with DAPI. Scale bar represents 200 µm.

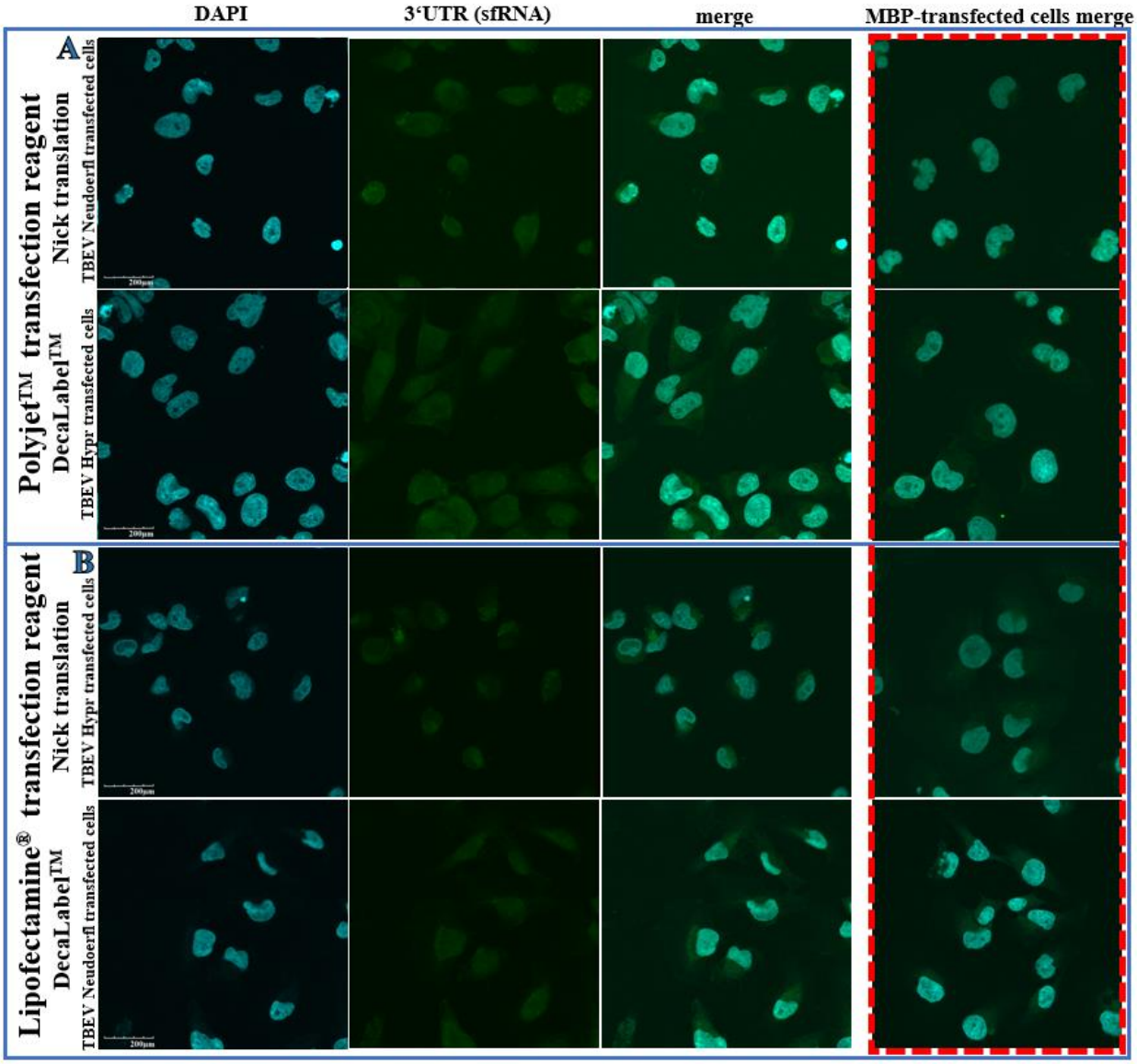

Figure 20: Direct FISH of DAOY HTB-186 cells transfected with *in vitro* transcribed sfRNA of TBEV Neudoerfl strain (N). **A)** DAOY cells were transfected using Polyjet™ *In vitro* DNA Transfection Reagent. FITC-labelled DNA probe (complementary to the 3'UTR (sfRNA) of TBEV (N) was prepared by nick translation or DecaLabel™ DNA Labelling kit. **B)** DAOY cells were transfected using Lipofectamine® RNAiMAX Transfection Reagent. FITC-labelled DNA probe (complementary to the 3'UTR (sfRNA) of TBEV (N) was prepared by nick translation or DecaLabel™ DNA Labelling kit. Nuclei were stained with DAPI. Scale bar represents 200 µm.

From the extensive optimisation alternatives, following results were observed:

- Polyjet^{TM} *In Vitro* DNA Transfection Reagent showed to be a slightly better option for transfection because the signal intensity of cells transfected with it was somewhat higher.

- The comparison of labelling methods (nick translation and random decamers of visualised signals showed that nick translation resulted in higher signal intensity and thus was more efficient for probe preparation.

- Direct fluorescence overall proved to be too insensitive for the detection of sfRNA in cells and was left out of further optimisation.

- The conspicuous signal difference between DIG-AntiDIG and Biotin-Streptavidin labelling resulted in the choice of Biotin-Streptavidin labelling for the optimal detection of cellular sfRNA. Biotin-Streptavidin detection proved to be not only more sensitive but created lower background in analysed slides and thus lead to more clarified imaging. Unfortunately, the first attempts of using Biotin-Streptavidin protocol led to the presence of high signal in all negative control samples (MBP-transfected cells) and therefore inconclusive analysis. This observation and studying literature show that neural cells express endogenous biotin (McKay *et al*., 2004). To prevent signal in negative control, biotin was blocked prior to hybridization using Avidin/Biotin Blocking Kit. Unfortunately, the signal difference between virus-infected and mock-infected cells was still inconclusive (results not shown).

- Additionally, several alternative fixation reagents were used for slides preparation (methanol, acetone, DSP and 4% paraformaldehyde for comparison). Data summarised in Figure 21 are representatives of only one experiment. Although only one experiment was performed for using different fixations, it is clear that DSP gave the best results concerning the signal intensity and specificity.

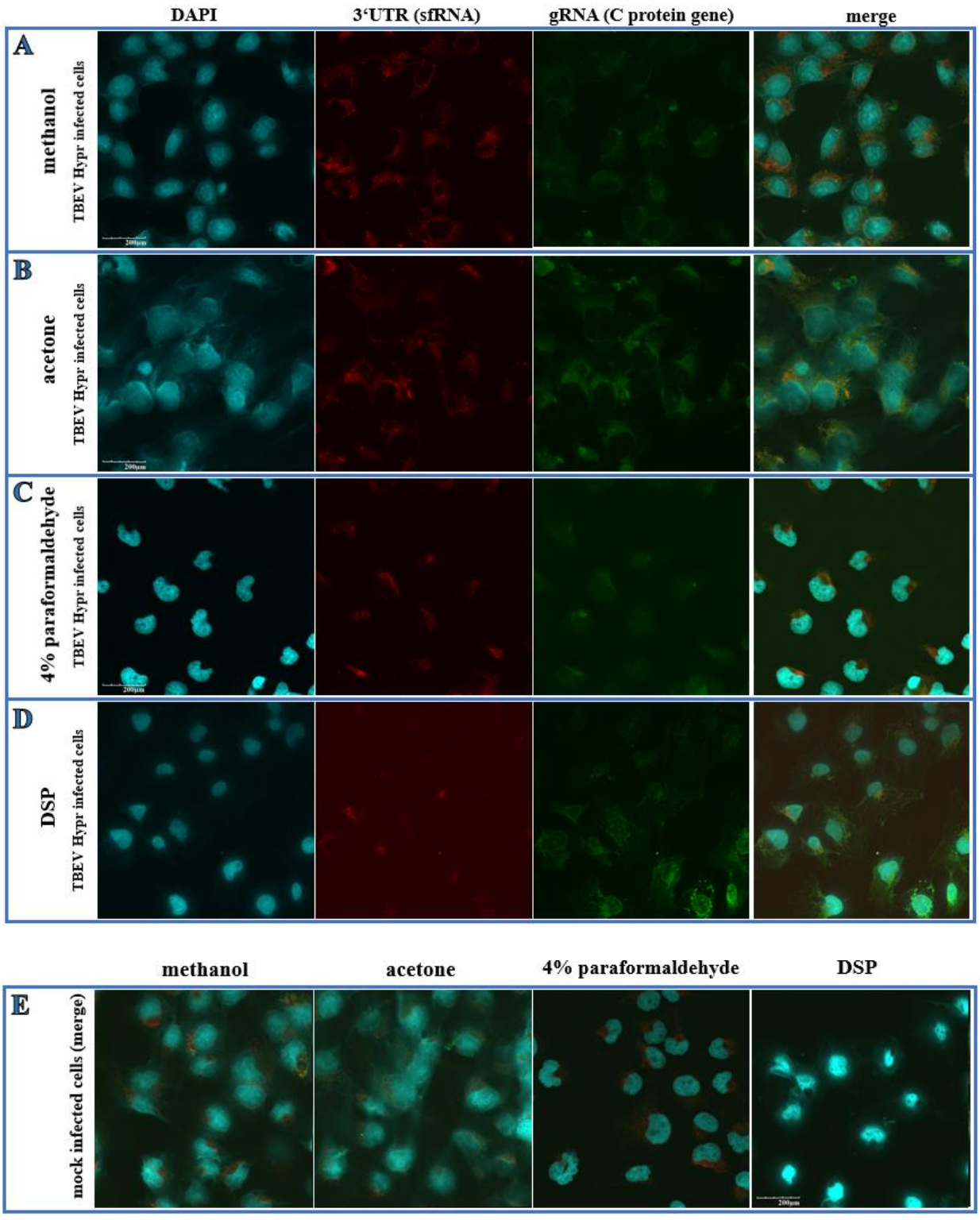

Figure 21: Indirect FISH of DAOY HTB-186 cells infected with TBEV Hypr strain. Biotinylated probe prepared using nick translation targeting the 3'UTR (sfRNA) of Hypr was visualised using Streptavidin DyLight® 549. DIG-labelled probe prepared using nick translation targeting gRNA (C protein gene) was

detected using Anti-DIG DyLight® 488. **A)** Cell fixated using methanol for 30 minutes at -20°C. **B)** Cells fixated using acetone for 30 minutes at -20°C. **C**) Cells fixated using 4% paraformaldehyde (ROTI® Histofix 4%, Roth) for 15 minutes at RT. **D**) Cells fixated using DSP for 30 minutes at RT. **E**) Mock infected cells fixated with selected fixation reagents. Nuclei were stained with DAPI. Scale bar represents 200 μm.

In conclusion, the optimal methodology for the localisation of sfRNA in transfected/infected cells has not been achieved yet and requires further experiments in the future. However, cells fixated with DSP show clear concentrated signal in detection of both gRNA and sfRNA, which would potentially serve as the best option for additional research.

6. Discussion

Flaviviruses represent a significant world-wide threat to public health as many of them cause severe neurological and haemorrhagic diseases in both humans and animals (Mackenzie *et al*., 2004). Unfortunately, no specific antiviral treatment has yet been developed so a thorough knowledge of flaviviral pathogenesis is necessary for further therapy research.

All flaviviruses tested to date have been discovered to corrupt host RNA degradation machinery for production of sfRNA (reviewed by Slonchak and Khromykh, 2018; MacFadden *et al*., 2018). This noncoding RNA further enhances flaviviral pathogenesis by retroactively inhibiting host and viral mRNA degradation, supressing type I INF response and RNAi response. Detailed functional studies of sfRNA have been focused predominantly on MBFs, so a more detailed look into the role of TBEV sfRNA has not yet been done before, although its presence has been confirmed (Schnettler *et al*., 2014).

Viruses have evolved ways to invade host translational machinery by several known mechanisms (inhibition of transcription initiation, induction of mRNA decay *etc*.) This unique ability ensures maximal viral gene expression and evasion of host immune response (Rampersad and Tennant, 2018). DENV (Roth *et al*., 2017; Reid *et al*., 2018) and ZIKV (Hou *et al*., 2017) have both been confirmed to reduce host protein production. The mechanism of translational shut-off during DENV infection has been characterized as ER remodelling and annexing strategy (Reid *et al*., 2018). ZIKV hijacks stress granule proteins (Hou *et al*., 2017), however, more detailed understanding for both flaviviruses is necessary. Furthermore, a recent study has shown that TBEV decreases the rate of *de novo* protein synthesis in host cells as well (Selinger *et al*., 2019), although the mechanism is still unclear.

In 2014, a novel insight into the role of sfRNA during DENV infection was observed by Bidet *et al*., 2014 – the DENV sfRNA was proved to supress specific host protein synthesis by downregulating mRNA translation of specific interferon-stimulated genes (ISGs). Similar observation was made by Manokaran *et al*. in 2015. Therefore, following the recent discoveries, the goal of this thesis was to explore whether the causative agent of translational shut-off in host cells during TBEV infection could be the sfRNA as well.

De novo synthesised proteins in cells transfected by *in vitro* transcribed sfRNA of DENV, ZIKV and TBEV (Neudoerfl and Hypr strains) were detected using Click-on-membrane chemistry assay (Kočová *et al*., in preparation). Interestingly, all sfRNAs tested were confirmed to supress host *de novo* protein synthesis. In the case of TBEV, the protein production was significantly lowered for both strains, however, Hypr strain showed more than 50% decrease, which corresponds to findings of Selinger *et al*., 2019. This observation could potentially relate to higher degree of virulence and neuroinvasivness which Hypr strain possesses.

The TBEV translational shut-off of host translation has also no effect on the translation of viral proteins (NS3 and C) which implies that the virus exploits translational shut-off for own benefit and is not affected by it (Selinger *et al*., 2019). This virus-induced non-specific translational shut-off is highly beneficial for the viral pathogenesis. For example, the reduction of host *de novo* protein synthesis during TBEV infection targeted production of ISGs such as viperin (Selinger *et al*., 2019), which was previously confirmed to participate in immune response against TBEV (Vonderstein *et al*., 2017; Panayiotou, *et al*., 2018). This indicates that sfRNA could play a role in regulation of these genes, too. In more detail, the sfRNA of DENV-2, which was studied by Bidet *et al*., (2014), was confirmed to bind to conserved host RNA-binding proteins - G3BP1, G3BP2, and CAPRIN1 and inactivate them. These RNA-binding proteins are required for the translation of mRNA of specific ISGs, namely PKR and IFITM2. On the contrary to DENV sfRNA, which was observed to target translation of specific genes (G3BP1, G3BP2, CAPRIN1 and TRIM25), our results show that TBEV sfRNA induces non-specific translational shut-off for the synthesis of host proteins.

There are many possible explanations to these observations which would need additional experiments for confirmation. As mentioned before, viruses inhibit eukaryotic protein synthesis by many mechanisms targeting transcriptional and translational pathways or supressing mRNA processing. Some viruses inhibit transcription initiation by either interfering with host transcription initiation factors (adenovirus; Dasgupta and Scovell, 2003) or function of host RNA polymerase II such as influenza virus (Vreede and Fodor, 2010). When hampering with host pre-mRNA processing, viruses were confirmed to induce mRNAs decay by their cleavage (SARS coronavirus; Huang *et al*., 2011), inhibition of nuclear export (rhinovirus, Ghildyal *et al*., 2009.) and inhibition of splicing or polyadenylation. Additionally, viruses also hinder host

translation pathways (such as ribosome shunting) for viral mRNA processing. sfRNA, being a small RNA species and targeting *de novo host* protein synthesis as a whole, can potentially possess any of these functions or operate on a completely different mechanism. Therefore, the mechanism remains unknown and demands further complex research.

Unlike the inhibition of host protein translation, virus-driven reduction of host rRNA is not as common, although it has been observed for several viruses, for example HIV (Ponti *et al*., 2008) or murine hepatitis virus (Banerjee *et al*., 2000). Host cells infected with DENV have been observed to have significantly annexed ER and adjacent ribosomes for the benefit of virion production, but 28S and 18S rRNA fractions were not affected (Reid *et al*., 2018). Furthermore, virus-induced inhibition of rRNA production has not been previously described for any other flaviviruses except TBEV (Selinger *et al*., 2019). TBEV hinders the production of 18S and 28S (both up to 50% decrease for TBEV Hypr strain) transcripts as well as 45-47S pre-rRNA in host cells. This observation was yet another inspiration for this thesis to determine whether the sfRNA could play a role in the inhibition of host rRNA synthesis.

De novo synthesised RNA of cells transfected *in vitro* transcribed sfRNA of DENV, ZIKV and TBEV (Neudoerfl and Hypr strains) was also detected using Click-on-membrane chemistry assay (Kočová *et al*., in preparation). However, the levels of newly synthesised rRNA were not overall conclusive and none of the selected sfRNAs contributed in a statistically significant decrease of host rRNA levels. These findings suggest that sfRNA acts specifically on the level of host translational inhibition.

Since the spatial distribution of translation (cytoplasm) and rRNA synthesis (nucleus) is different, our next goal was to determine the localisation of sfRNA, which may further support our findings. Therefore, the last part of this thesis was focused on the localisation of TBEV sfRNA of in transfected/infected DAOY HTB-186 cells. Fluorescence *in situ* hybridization was chosen for the detection as it was successfully performed with TBEV-infected neurons in the past (Hirano *et al*., 2014) and it was also used for sfRNA detection in WNV-infected cells (Pijlman *et al*., 2008). However, the first step of successful localisation method was to find optimal transfecting, fixating and labelling conditions. Following transfection optimisation, further experiments were also conducted on TBEV-infected cells. To distinguish sfRNA (3’UTR) from the localisation of

3’UTR region of viral gRNA, we employed two differently labelled DNA probes complementary to the sfRNA and a C protein gene of TBEV.

When transfecting cells in previous protocols in this thesis, Polyjet™ *In vitro* DNA Transfection Reagent was used. However, for further investigation, additional transfection reagent - Lipofectamine® RNAiMAX Transfection Reagent - was picked for examination, since it is specially designed for the endocytic transport of small RNA species and similar Lipofectamine transfection reagent was used by Schnettler *et al*., 2014. Eventually, the results obtained were comparable between the two reagents with a higher and more specific signal in Polyjet-transfected cells which confirmed Polyjet reagent to be slightly more efficient.

A DNA probe prepared by PCR was labelled using two distinct protocols to compare labelling efficiency (random decamers and nick translation). The protocol for nick translation labelling was adapted from Kato *et al*., 2006 and in the end resulted in higher signal quality.

The DNA probe was labelled using one direct (FITC) and two different indirect labelling systems (DIG/Anti-DIG and Biotin/Streptavidin). As expected, direct fluorescence was not sensitive enough to provide almost any signal. A higher sensitivity was observed when using indirect fluorescence, however, DIG/Anti-DIG labelling system resulted in a rather unfocused signal with high background.

When using biotinylated DNA probes for the detection of sfRNA, an unexpected trouble occurred while visualising signals with Streptavidin DyLight® 549. The signal intensity was equal in TBEV- and MBP-transfected cells (as well as TBEV- and mock- infected), which yielded inconclusive results. Adjusted upon reading literature (McKay *et al*., 2004), the endogenously expressed biotin in DAOY HTB-186 cells, which could potentially amplify the signal, was blocked. Unfortunately, the signal difference in following experiments which included the blocking of endogenous biotin, led to the same issue. Following these results, a different approach was used in order to potentially break the conserved secondary structures in the 3’UTR region, which could have been possibly stabilized by the fixation with paraformaldehyde and thus, led to incomplete hybridization. Therefore, we employed three different fixative agents working on a different principle of fixation: methanol, acetone, and DSP.

Methanol and acetone are organic fixation reagents which work through a process of dehydration and precipitation of proteins and are widely used in histology (reviewed by Hobro and Smith, 2017). These two fixation agents were included in the optimisation experiments of fixation, as they would potentially lead to the disruption of complex secondary structures holding sfRNA and thus better accessibility for hybridization. However, they both resulted in the damage of membrane structures, slight loss of nuclear content and were not optimal fixation reagents overall because the signal in mock infected cells was still comparable to TBEV infected cells as well.

A membrane-permeable cross-linker was selected as a third alternative to initial paraformaldehyde fixation to avoid potential autofluorescence in fixated cells and to generally improve the signal. Unlike methanol and acetone, cross-linking is a less toxic fixative which results in efficient cell and tissue anchoring. Results obtained from confocal microscopy from slides fixated using a DSP cross-linker showed to be the most conclusive throughout all other optimisation experiments. The gRNA signal was concentrated in the cytoplasmic part of the cells, with its localisation presumably in the ER surrounding the nuclei. Cross-linking additionally provided the clearest signal of sfRNA with no signal occurrence in mock-infected cells. This reagent was proved to serve as the optimal fixation technique compared to the rest, however, the results obtained are from one experiment. For additional confirmation of this conclusion, further experiments are needed to be done in the future.

sfRNA localisation has been successfully pinpointed in WNV-infected cells to the sites of cytoplasmic processing bodies by Pijlman *et al*., 2008. However, further localisation investigation has not yet been concluded for other flaviviruses. The localisation of TBEV sfRNA in cells during ongoing TBEV infection faces several challenging problems from which some of them have been resolved by this thesis.

Unlike the sfRNA of other flaviviruses, very little is known about the functions of TBEV sfRNA. In conclusion, this thesis brings more detailed look into the role of sfRNA in host cells and additionally provides complex information for forthcoming experiments.

7. Conclusion

In conclusion, this thesis provides further insight into the functions of sfRNA during TBEV infection of which is very little known. The sfRNA of TBEV (Hypr and Neudoerfl strains) has been confirmed to decrease *de novo* host protein synthesis, with Hypr strain inhibiting the synthesis by more than 50%.

On the other hand, the correlation between sfRNA presence and the downregulation of host rRNA *de novo* synthesis has not been found. None of four flaviviruses tested (DENV, ZIKV, TBEV (Hypr and Neudoerfl strains) showed significant decrease of *de novo* synthesised host rRNA.

Furthermore, this thesis provides a complex insight into the optimisation of fluorescence *in situ* hybridization technique for the localisation of TBEV sfRNA in host cells, which can be used as a helpful tool for further research.

8. List of abbreviations

5-EU	5-Ethynyl Uridine
AHA	4-Azido-L-homoalanine
APS	ammonium persulfate
arboviruses	arthropod-borne viruses
BBB	blood-brain barrier
bp	base pairs
BSA	bovine serum albumin
C protein	capsid protein
C_t	cycle threshold
CMV	cytomegalovirus
DAOY	human desmoplastic cerebellar medulloblastoma cell line
DAPI	4',6-diamidin-2-fenylindol
DB	dumbbell
DENV	dengue virus
DEPC	diethyl pyrocarbonate
dH_2O	distilled water
DIG	digoxigenin-11-dUTP
DNA	deoxyribonucleic acid
dNTP	deoxynucleotide
dsDNA	double stranded DNA
DSP	dithiobis(succinimidyl propionate)
dUTP	2'-deoxyuridine-5'-triphosphate
E protein	envelope protein
ER	endoplasmic reticulum
FBS	fetal bovine serum
FISH	fluorescence *in situ* hybridization
FITC	fluorescein-12-dUTP
gRNA	genomic RNA
HDVr	hepatitis delta virus ribozyme
HPG	L-Homopropargylglycine
HPRT1	hypoxanthine phosphoribosyltransferase 1
p.t.	post transfection
IFN	interferon
IFNα	interferon alpha
IL-1β	interleukin 1 beta
IL-6	interleukin 6
IL-8	interleukin 8
IL-10	interleukin 10
JEV	japanese encephalitis virus

kDa	kilodalton
LGTV	langat virus
M protein	membrane protein
MBP	maltose-binding protein
MBFs	mosquito-borne flaviviruses
MHC	major histocompatibility complex
mRNA	messenger RNA
MVE	Murray Valley encephalitis virus
NS	non-structural
nt	nucleotide
NTP	nucleoside triphosphate
ORF	open reading frame
PBS	phosphate buffered saline
PK	pseudoknot
prM protein	precursor membrane protein
PVDF	polyvinylidene difluoride
qRT-PCR	quantitative reverse transcription polymerase chain reaction
RNA	ribonucleic acid
RNAi	RNA interference
rRNA	ribosomal RNA
RT	room temperature
SDS	sodium dodecyl sulfate
sfRNA	subgenomic flaviviral RNA
SL	stem-loop
SSC	saline-sodium citrate
TAE	Tris-acetate-EDTA buffer
TBE	tick-borne encephalitis
TBEV	tick-borne encephalitis virus
TBFs	tick-borne flaviviruses
TEMED	tetramethylethylendiamin
THPTA	tris-hydroxypropyltriazolylmethylamine
TNF-α	tumour necrosis factor alpha
UTR	untranslated region
WHO	World Health Organisation
WNV	West Nile virus
wt	wild type
XRN1	5'-3' exoribonuclease 1
xrRNA	XRN1-resistant RNA
YFV	yellow fever virus
ZIKV	zika virus

9. References

Agarwal, P., Beahm, B. J., Shieh, P., & Bertozzi, C. R. (2015). **Systemic Fluorescence Imaging of Zebrafish Glycans with Bioorthogonal Chemistry**. *Angewandte Chemie International Edition*, ***54***(39), 11504–11510. https://doi.org/10.1002/anie.201504249

Agumadu, V. C., & Ramphul, K. (2018). **Zika Virus: A Review of Literature**. *Cureus*, ***10(7)***, e3025. https://doi.org/10.7759/cureus.3025

Akiyama, B. M., Laurence, H. M., Massey, A. R., Costantino, D. A., Xie, X., Yang, Y., Shi, P.-Y., Nix, J. C., Beckham, J. D., & Kieft, J. S. (2016). **Zika virus produces noncoding RNAs using a multi-pseudoknot structure that confounds a cellular exonuclease**. *Science*, ***354***(6316), 1148–1152. https://doi.org/10.1126/science.aah3963

Banerjee, S., An, S., Zhou, A., Silverman, R. H., & Makino, S. (2000). **RNase L-Independent Specific 28S rRNA Cleavage in Murine Coronavirus-Infected Cells**. *Journal of Virology*, ***74***(19), 8793–8802. https://doi.org/10.1128/jvi.74.19.8793-8802.2000

Barrett, A. D. T., & Teuwen, D. E. (2009). **Yellow fever vaccine—how does it work and why do rare cases of serious adverse events take place?** *Current Opinion in Immunology*, ***21***(3), 308–313. https://doi.org/10.1016/j.coi.2009.05.018

Barrows, N. J., Campos, R. K., Liao, K.-C., Prasanth, K. R., Soto-Acosta, R., Yeh, S.-C., Schott-Lerner, G., Pompon, J., Sessions, O. M., Bradrick, S. S., & Garcia-Blanco, M. A. (2018). **Biochemistry and Molecular Biology of Flaviviruses**. *Chemical Reviews*, ***118***(8), 4448–4482. https://doi.org/10.1021/acs.chemrev.7b00719

Bernstein, E., Caudy, A. A., Hammond, S. M., & Hannon, G. J. (2001). **Role for a bidentate ribonuclease in the initiation step of RNA interference**. *Nature*, ***409***(6818), 363–366. https://doi.org/10.1038/35053110

Bidet, K., Dadlani, D., & Garcia-Blanco, M. A. (2014). **G3BP1, G3BP2 and CAPRIN1 Are Required for Translation of Interferon Stimulated mRNAs and Are Targeted by a Dengue Virus Non-coding RNA**. *PLOS Pathogens*, ***10***(7), e1004242. https://doi.org/10.1371/journal.ppat.1004242

Boldescu, V., Behnam, M. A. M., Vasilakis, N., & Klein, C. D. (2017). **Broad-spectrum agents for flaviviral infections: dengue, Zika and beyond**. *Nature Reviews Drug Discovery*, ***16***(8), 565–586. https://doi.org/10.1038/nrd.2017.33

Bowie, A. G., & Fitzgerald, K. A. (2007). **RIG-I: tri-ing to discriminate between self and non-self RNA**. *Trends in Immunology*, ***28***(4), 147–150. https://doi.org/10.1016/j.it.2007.02.002

Bowman, A. S., Ball, A., & Sauer, J. R. (2008). **Tick salivary glands: the physiology of tick water balance and their role in pathogen trafficking and transmission**. *Ticks*, **7**(281), 73–91. https://doi.org/10.1017/cbo9780511551802.004

Brinton, M. A., Fernandez, A. V., & Dispoto, J. H. (1986). **The 3′-nucleotides of flavivirus genomic RNA form a conserved secondary structure**. *Virology*, ***153***(1), 113–121. https://doi.org/10.1016/0042-6822(86)90012-7

Burke D.S. and Monath, T. P. (2001) **Flaviviruses.** In Knipe, D.M. and Howley, P.M., *Fields Virology*. Lippincott-Williams & Wilkins, Philadelphia, PA, 1043–1125

Cao-Lormeau, V.-M. (2009). **Dengue viruses binding proteins from Aedes aegypti and Aedes polynesiensis salivary glands**. *Virology Journal*, ***6***(1), 35. https://doi.org/10.1186/1743-422x-6-35

Chambers, T. J., & Diamond, M. S. (2003). **Pathogenesis of flavivirus encephalitis**. *Advances in Virus Research*, ***60***, 273–342. https://doi.org/10.1016/s0065-3527(03)60008-4

Chang, R.-Y., Hsu, T.-W., Chen, Y.-L., Liu, S.-F., Tsai, Y.-J., Lin, Y.-T., Chen, Y.-S., & Fan, Y.-H. (2013). **Japanese encephalitis virus non-coding RNA inhibits activation of interferon by blocking nuclear translocation of interferon regulatory factor 3**. *Veterinary Microbiology*, ***166***(1–2), 11–21. https://doi.org/10.1016/j.vetmic.2013.04.026

Chapman, E. G., Costantino, D. A., Rabe, J. L., Moon, S. L., Wilusz, J., Nix, J. C., & Kieft, J. S. (2014). **The Structural Basis of Pathogenic Subgenomic Flavivirus RNA (sfRNA) Production**. *Science*, ***344***(6181), 307–310. https://doi.org/10.1126/science.1250897

Chen, Y., Maguire, T., Hileman, R. E., Fromm, J. R., Esko, J. D., Linhardt, R. J., & Marks, R. M. (1997). **Dengue virus infectivity depends on envelope protein binding to target cell heparan sulfate**. *Nature Medicine*, ***3***(8), 866–871. https://doi.org/10.1038/nm0897-866

Choi, K. H., Groarke, J. M., Young, D. C., Kuhn, R. J., Smith, J. L., Pevear, D. C., & Rossmann, M. G. (2004). **The structure of the RNA-dependent RNA polymerase from bovine viral diarrhea virus establishes the role of GTP in *de novo* initiation**. *Proceedings of the National Academy of Sciences*, ***101***(13), 4425–4430. https://doi.org/10.1073/pnas.0400660101

Christofferson, R. C. (2016). **Zika Virus Emergence and Expansion: Lessons Learned from Dengue and Chikungunya May Not Provide All the Answers**. *The American Journal of Tropical Medicine and Hygiene*, ***95***(1), 15–18. https://doi.org/10.4269/ajtmh.15-0866

Ciota, A. T., Bialosuknia, S. M., Ehrbar, D. J., & Kramer, L. D. (2017). **Vertical Transmission of Zika Virus by *Aedes aegypti* and *Ae. Albopictus* mosquitoes**. *Emerging Infectious Diseases*, ***23***(5), 880–882. https://doi.org/10.3201/eid2305.162041

Clarke, B. D., Roby, J. A., Slonchak, A., & Khromykh, A. A. (2015). **Functional non-coding RNAs derived from the flavivirus 3′ untranslated region**. *Virus Research*, ***206***, 53–61. https://doi.org/10.1016/j.virusres.2015.01.026

Danielová, V., Holubová. (1991). **Transovarial transmission rate of tick-borne encephalitis virus in *Ixodes ricinus* ticks**. *Modern Acarology*, ***2***. Academia Prague and SPB Academic Publishing, 7-10.

Dasgupta, A., & Scovell, W. M. (2003). **TFIIA abrogates the effects of inhibition by HMGB1 but not E1A during the early stages of assembly of the transcriptional preinitiation complex**. *Biochimica et Biophysica Acta (BBA) - Gene Structure and Expression*, ***1627***(2–3), 101–110. https://doi.org/10.1016/s0167-4781(03)00080-0

Diamond, M. S., & Gale, M. (2012). **Cell-intrinsic innate immune control of West Nile virus infection**. *Trends in Immunology*, ***33***(10), 522–530. https://doi.org/10.1016/j.it.2012.05.008

Dick, G. W. A. (1952). **Zika virus (II). Pathogenicity and physical properties**. *Transactions of the Royal Society of Tropical Medicine and Hygiene*, ***46***(5), 521–534. https://doi.org/10.1016/0035-9203(52)90043-6

Donald, C. L., Brennan, B., Cumberworth, S. L., Rezelj, V. V., Clark, J. J., Cordeiro, M. T., Freitas de Oliveira França, R., Pena, L. J., Wilkie, G. S., Da Silva Filipe, A., Davis, C., Hughes, J., Varjak, M., Selinger, M., Zuvanov, L., Owsianka, A. M., Patel, A. H., McLauchlan, J., Lindenbach, B. D., & Kohl, A. (2016). **Full Genome Sequence and sfRNA Interferon Antagonist Activity of Zika Virus from Recife, Brazil**. *PLOS Neglected Tropical Diseases*, ***10***(10), e0005048. https://doi.org/10.1371/journal.pntd.0005048

Ecker, M., Allison, S. L., Meixner, T., & Heinz, F. X. (1999). **Sequence analysis and genetic classification of tick-borne encephalitis viruses from Europe and Asia**. *Journal of General Virology*, ***80***(1), 179–185. https://doi.org/10.1099/0022-1317-80-1-179

Elrefaey, A. M. E., Abdelnabi, R., Rosales Rosas, A. L., Wang, L., Basu, S., & Delang, L. (2020). **Understanding the Mechanisms Underlying Host Restriction of Insect-Specific Viruses**. *Viruses*, ***12***(9), 964. https://doi.org/10.3390/v12090964

Filomatori, C. V. (2006). **A 5' RNA element promotes dengue virus RNA synthesis on a circular genome**. *Genes & Development*, ***20***(16), 2238–2249. https://doi.org/10.1101/gad.1444206

Filomatori, C. V., Carballeda, J. M., Villordo, S. M., Aguirre, S., Pallarés, H. M., Maestre, A. M., Sánchez-Vargas, I., Blair, C. D., Fabri, C., Morales, M. A., Fernandez-Sesma, A., & Gamarnik, A. V. (2017). **Dengue virus genomic variation associated with mosquito adaptation defines the pattern of viral non-coding RNAs and fitness in human cells**. *PLOS Pathogens*, ***13***(3), e1006265. https://doi.org/10.1371/journal.ppat.1006265

Foy, B. D., Kobylinski, K. C., Foy, J. L. C., Blitvich, B. J., Travassos da Rosa, A., Haddow, A. D., Lanciotti, R. S., & Tesh, R. B. (2011). **Probable Non–Vector-borne Transmission of Zika Virus, Colorado, USA**. *Emerging Infectious Diseases*, ***17***(5), 880–882. https://doi.org/10.3201/eid1705.101939

Friebe, P., Peña, J., Pohl, M. O. F., & Harris, E. (2012). **Composition of the sequence downstream of the dengue virus 5′ cyclization sequence (dCS) affects viral RNA replication**. *Virology*, ***422***(2), 346–356. https://doi.org/10.1016/j.virol.2011.10.025

Fritz, R., Orlinger, K. K., Hofmeister, Y., Janecki, K., Traweger, A., Perez-Burgos, L., Barrett, P. N., & Kreil, T. R. (2012). **Quantitative comparison of the cross-protection induced by tick-borne encephalitis virus vaccines based on European and Far Eastern virus subtypes**. *Vaccine*, ***30***(6), 1165–1169. https://doi.org/10.1016/j.vaccine.2011.12.013

Funk, A., Truong, K., Nagasaki, T., Torres, S., Floden, N., Balmori Melian, E., Edmonds, J., Dong, H., Shi, P.-Y., & Khromykh, A. A. (2010). **RNA Structures Required for Production of Subgenomic Flavivirus RNA**. *Journal of Virology*, ***84***(21), 11407–11417. https://doi.org/10.1128/jvi.01159-10

Garcia-Blanco, M. A., Vasudevan, S. G., Bradrick, S. S., & Nicchitta, C. (2016). **Flavivirus RNA transactions from viral entry to genome replication**. *Antiviral Research*, ***134***, 244–249. https://doi.org/10.1016/j.antiviral.2016.09.010

Gaunt, M. W., Sall, A. A., Lamballerie, X., Falconar, A. K. I., Dzhivanian, T. I., & Gould, E. A. (2001). **Phylogenetic relationships of flaviviruses correlate with their epidemiology, disease association and biogeography**. *Journal of General Virology*, ***82***(8), 1867–1876. https://doi.org/10.1099/0022-1317-82-8-1867

Gebhard, L. G., Filomatori, C. V., & Gamarnik, A. V. (2011). **Functional RNA Elements in the Dengue Virus Genome**. *Viruses*, ***3***(9), 1739–1756. https://doi.org/10.3390/v3091739

Ghildyal, R., Jordan, B., Li, D., Dagher, H., Bardin, P. G., Gern, J. E., & Jans, D. A. (2009). **Rhinovirus 3C Protease Can Localize in the Nucleus and Alter Active and Passive Nucleocytoplasmic Transport**. *Journal of Virology*, ***83***(14), 7349–7352. https://doi.org/10.1128/jvi.01748-08

Gillespie, L. K., Hoenen, A., Morgan, G., & Mackenzie, J. M. (2010). **The Endoplasmic Reticulum Provides the Membrane Platform for Biogenesis of the Flavivirus Replication Complex**. *Journal of Virology*, ***84***(20), 10438–10447. https://doi.org/10.1128/jvi.00986-10

Gokhale, N. S., McIntyre, A. B. R., McFadden, M. J., Roder, A. E., Kennedy, E. M., Gandara, J. A., Hopcraft, S. E., Quicke, K. M., Vazquez, C., Willer, J., Ilkayeva, O. R., Law, B. A., Holley, C. L., Garcia-Blanco, M. A., Evans, M. J., Suthar, M. S., Bradrick, S. S., Mason, C. E., & Horner, S. M. (2016). **N6 -Methyladenosine in Flaviviridae Viral RNA Genomes Regulates Infection**. *Cell Host & Microbe*, ***20***(5), 654–665. https://doi.org/10.1016/j.chom.2016.09.015

Göertz, G. P., Abbo, S. R., Fros, J. J., & Pijlman, G. P. (2018). **Functional RNA during Zika virus infection**. *Virus Research*, ***254***, 41–53. https://doi.org/10.1016/j.virusres.2017.08.015

Gritsun, T. S., Lashkevich, V. A., & Gould, E. A. (2003). **Tick-borne encephalitis**. *Antiviral Research*, ***57***(1–2), 129–146. https://doi.org/10.1016/s0166-3542(02)00206-1

Gubler D J. (1988). **Dengue**. *Epidemiology of arthropod-borne viral diseases*. Boca Raton, Fla: CRC Press, Inc., 223–260.

Gubler, D. J. (1998). **Dengue and Dengue Hemorrhagic Fever**. *Clinical Microbiology Reviews*, ***11***(3), 480–496. https://doi.org/10.1128/cmr.11.3.480

Hall, N. B., Broussard, K., Evert, N., & Canfield, M. (2017). **Notes from the Field: Zika Virus-Associated Neonatal Birth Defects Surveillance — Texas, January 2016–July 2017**. *MMWR. Morbidity and Mortality Weekly Report*, ***66***(31), 835–836. https://doi.org/10.15585/mmwr.mm6631a5

Halstead S. B. (1988). **Pathogenesis of dengue: challenges to molecular biology**. *Science*, ***239***, 476–481.

Hasan, S., Jamdar, S. F., Alalowi, M., & Al Ageel Al Beaiji, S. M. (2016). **Dengue virus: A global human threat: Review of literature**. *Journal of International Society of Preventive and Community Dentistry*, ***6***(1), 1-6. https://doi.org/10.4103/2231-0762.175416

Heinz, F. X. (1986). **Epitope Mapping of Flavivirus Glycoproteins**. *Advances in Virus Research*, ***31***, 103–168. https://doi.org/10.1016/s0065-3527(08)60263-8

Heinz, F. X., & Allison, S. L. (2003). **Flavivirus Structure and Membrane Fusion**. *Advances in Virus Research*, ***59***, 63–97. https://doi.org/10.1016/s0065-3527(03)59003-0

Heinz, F. X., & Stiasny, K. (2012). **Flaviviruses and flavivirus vaccines**. *Vaccine*, ***30***(29), 4301–4306. https://doi.org/10.1016/j.vaccine.2011.09.114

Henchal, E. A., & Putnak, J. R. (1990). **The dengue viruses**. *Clinical Microbiology Reviews*, ***3***(4), 376–396. https://doi.org/10.1128/cmr.3.4.376

Hennessey, M., Fischer, M., & Staples, J. E. (2016). **Zika Virus Spreads to New Areas — Region of the Americas, May 2015–January 2016**. *MMWR. Morbidity and Mortality Weekly Report*, ***65***(3), 55–58. https://doi.org/10.15585/mmwr.mm6503e1

Hirano, M., Muto, M., Sakai, M., Kondo, H., Kobayashi, S., Kariwa, H., & Yoshii, K. (2017). **Dendritic transport of tick-borne flavivirus RNA by neuronal granules affects development of neurological disease**. *Proceedings of the National Academy of Sciences*, ***114***(37), 9960–9965. https://doi.org/10.1073/pnas.1704454114

Hirano, M., Yoshii, K., Sakai, M., Hasebe, R., Ichii, O., & Kariwa, H. (2014). **Tick-borne flaviviruses alter membrane structure and replicate in dendrites of primary mouse neuronal cultures**. *Journal of General Virology*, ***95***(4), 849–861. https://doi.org/10.1099/vir.0.061432-0

Hobro, A. J., & Smith, N. I. (2017). **An evaluation of fixation methods: Spatial and compositional cellular changes observed by Raman imaging**. *Vibrational Spectroscopy*, ***91***, 31–45. https://doi.org/10.1016/j.vibspec.2016.10.012

Hou, S., Kumar, A., Xu, Z., Airo, A. M., Stryapunina, I., Wong, C. P., Branton, W., Tchesnokov, E., Götte, M., Power, C., & Hobman, T. C. (2017). **Zika Virus Hijacks Stress Granule Proteins and Modulates the Host Stress Response**. *Journal of Virology*, ***91***(16), e00474-17. https://doi.org/10.1128/jvi.00474-17

Huang, C., Lokugamage, K. G., Rozovics, J. M., Narayanan, K., Semler, B. L., & Makino, S. (2011). **SARS Coronavirus nsp1 Protein Induces Template-Dependent Endonucleolytic Cleavage of mRNAs: Viral mRNAs Are Resistant to nsp1-Induced RNA Cleavage**. *PLOS Pathogens*, ***7***(12), e1002433. https://doi.org/10.1371/journal.ppat.1002433

Huisgen, R. (1963). **1,3-Dipolar Cycloadditions. Past and Future**. *Angewandte Chemie International Edition in English*, ***2***(10), 565–598. https://doi.org/10.1002/anie.196305651

Jacobsen, P. F., Jenkyn, D. J., & Papadimitriou, J. M. (1985). **Establishment of a Human Medulloblastoma Cell Line and Its Heterotransplantation into Nude Mice**. *Journal of Neuropathology and Experimental Neurology*, ***44***(5), 472–485. https://doi.org/10.1097/00005072-198509000-00003

Kato, A., Albert, P. S., Vega, J. M., Kato, A., Albert, P. S., Vega, J. M., & Birchler, J. A. (2006). **Sensitive fluorescence*in situ*hybridization signal detection in maize using directly labeled probes produced by high concentration DNA polymerase nick translation**. *Biotechnic & Histochemistry*, ***81***(2–3), 71–78. https://doi.org/10.1080/10520290600643677

Kaufman, W. R., & Nuttall, P. A. (1996). ***Amblyomma variegatum* (Acari: *Ixodidae*): Mechanism and Control of Arbovirus Secretion in Tick Saliva**. *Experimental Parasitology*, ***82***(3), 316–323. https://doi.org/10.1006/expr.1996.0039

Khasnatinov, M. A., Tuplin, A., Gritsun, D. J., Slovak, M., Kazimirova, M., Lickova, M., Havlikova, S., Klempa, B., Labuda, M., Gould, E. A., & Gritsun, T. S. (2016). **Tick-Borne Encephalitis Virus Structural Proteins Are the Primary Viral Determinants of Non-Viraemic Transmission between Ticks whereas Non-Structural Proteins Affect Cytotoxicity**. *PLOS ONE*, ***11***(6), e0158105. https://doi.org/10.1371/journal.pone.0158105

Kieft, J. S., Rabe, J. L., & Chapman, E. G. (2015). **New hypotheses derived from the structure of a flaviviral Xrn1-resistant RNA: Conservation, folding, and host adaptation**. *RNA Biology*, ***12***(11), 1169–1177. https://doi.org/10.1080/15476286.2015.1094599

Kunz C, Hofmann H, Stary A. (1976). **Field studies with a new tick-borne encephalitis (TBE) vaccine**. *Zentralbl Bakteriol Orig A.*, **234**, 141–144.

Korhonen, E. M., Huhtamo, E., Smura, T., Kallio-Kokko, H., Raassina, M., & Vapalahti, O. (2016). **Zika virus infection in a traveller returning from the Maldives, June 2015**. *Eurosurveillance*, ***21***(2), 2-5. https://doi.org/10.2807/1560-7917.es.2016.21.2.30107

Kuhn, R. J., Dowd, K. A., Beth Post, C., & Pierson, T. C. (2015). **Shake, rattle, and roll: Impact of the dynamics of flavivirus particles on their interactions with the host**. *Virology*, ***479–480***, 508–517. https://doi.org/10.1016/j.virol.2015.03.025

Kuhn, R. J., Zhang, W., Rossmann, M. G., Pletnev, S. V., Corver, J., Lenches, E., Jones, C. T., Mukhopadhyay, S., Chipman, P. R., Strauss, E. G., Baker, T. S., & Strauss, J. H. (2002). **Structure of Dengue Virus**. *Cell*, ***108***(5), 717–725. https://doi.org/10.1016/s0092-8674(02)00660-8

Kuno, G., Chang, G.-J. J., Tsuchiya, K. R., Karabatsos, N., & Cropp, C. B. (1998). **Phylogeny of the Genus Flavivirus**. *Journal of Virology*, ***72***(1), 73–83. https://doi.org/10.1128/jvi.72.1.73-83.1998

Labuda, M., Austin, J. M., Zuffova, E., Kozuch, O., Fuchsberger, N., Lysy, J., & Nuttall, P. A. (1996). **Importance of Localized Skin Infection in Tick-Borne Encephalitis Virus Transmission**. *Virology*, ***219***(2), 357–366. https://doi.org/10.1006/viro.1996.0261

Labuda, M., Kozuch, O., Zuffová, E., Elecková, E., Hails, R. S., & Nuttall, P. A. (1997). **Tick-Borne Encephalitis Virus Transmission between Ticks Cofeeding on Specific Immune Natural Rodent Hosts**. *Virology*, ***235***(1), 138–143. https://doi.org/10.1006/viro.1997.8622

Lefkowitz, E. J., Dempsey, D. M., Hendrickson, R. C., Orton, R. J., Siddell, S. G., & Smith, D. B. (2017). **Virus taxonomy: the database of the International Committee on Taxonomy of Viruses (ICTV)**. *Nucleic Acids Research*, ***46***(D1), D708–D717. https://doi.org/10.1093/nar/gkx932

Lehrer, A. T., & Holbrook, M. R. (2011). **Tick-borne Encephalitis Vaccines**. *Journal of Bioterrorism & Biodefense*, ***2011 (Suppl. 1)***, ***3***. https://doi.org/10.4172/2157-2526.s1-003

Lilley, D. M. J. (1998). **Folding of branched RNA species**. *Biopolymers*, ***48***(2–3), 101–112. https://doi.org/10.1261/rna.2208106

Lin, K.-C., Chang, H.-L., & Chang, R.-Y. (2004). **Accumulation of a 3′-Terminal Genome Fragment in Japanese Encephalitis Virus-Infected Mammalian and Mosquito Cells**. *Journal of Virology*, ***78***(10), 5133–5138. https://doi.org/10.1128/jvi.78.10.5133-5138.2004

Lindenbach BD, Murray CL, Thiel HJ, Rice CM. (2013). **Flaviviviridae.** In: Knipe DM. *Fields Virology*. Philadelphia: Lippincott Williams & Wilkins; 712–746

Lindenbach, B. D., & Rice, C. M. (2003). **Molecular biology of flaviviruses**. *Advances in Virus Research*, ***277***, 23–61. https://doi.org/10.1016/s0065-3527(03)59002-9

Lindquist, L., & Vapalahti, O. (2008). **Tick-borne encephalitis**. *The Lancet*, ***371***(9627), 1861–1871. https://doi.org/10.1016/s0140-6736(08)60800-4

Linthicum I, K. J., Platt, K., Myint, K. S., Lerdthusnee, K., Inni, B. L., & Ghn, D. W. V. A. U. (1996). **Dengue 3 virus distribution in the mosquito Aedes aegypti: an immunocytochemical study**. *Medical and Veterinary Entomology*, ***10***(1), 87–92. https://doi.org/10.1111/j.1365-2915.1996.tb00086.x

Liu, R., Yue, L., Li, X., Yu, X., Zhao, H., Jiang, Z., Qin, E., & Qin, C. (2010). **Identification and characterization of small sub-genomic RNAs in dengue 1–4 virus-infected cell cultures and tissues**. *Biochemical and Biophysical Research Communications*, ***391***(1), 1099–1103. https://doi.org/10.1016/j.bbrc.2009.12.030

Lodeiro, M.́. F., Filomatori, C. V., & Gamarnik, A. V. (2008). **Structural and Functional Studies of the Promoter Element for Dengue Virus RNA Replication**. *Journal of Virology*, ***83***(2), 993–1008. https://doi.org/10.1128/jvi.01647-08

Ma, L., Jones, C. T., Groesch, T. D., Kuhn, R. J., & Post, C. B. (2004). **Solution structure of dengue virus capsid protein reveals another fold**. *Proceedings of the National Academy of Sciences*, ***101***(10), 3414–3419. https://doi.org/10.1073/pnas.0305892101

MacFadden, A., O'Donoghue, Z., Silva, P. A. G. C., Chapman, E. G., Olsthoorn, R. C., Sterken, M. G., Pijlman, G. P., Bredenbeek, P. J., & Kieft, J. S. (2018). **Mechanism and structural diversity of exoribonuclease-resistant RNA structures in flaviviral RNAs**. *Nature Communications*, ***9***(1), 119. https://doi.org/10.1038/s41467-017-02604-y

Mackenzie, J. (2005). **Wrapping Things up about Virus RNA Replication**. *Traffic*, ***6***(11), 967–977. https://doi.org/10.1111/j.1600-0854.2005.00339.x

Mackenzie, J. M., Khromykh, A. A., Jones, M. K., & Westaway, E. G. (1998). **Subcellular Localization and Some Biochemical Properties of the Flavivirus Kunjin Nonstructural Proteins NS2A and NS4A**. *Virology*, ***245***(2), 203–215. https://doi.org/10.1006/viro.1998.9156

Mackenzie, J. S., Gubler, D. J., & Petersen, L. R. (2004). **Emerging flaviviruses: the spread and resurgence of Japanese encephalitis, West Nile and dengue viruses**. *Nature Medicine*, ***10***(S12), S98–S109. https://doi.org/10.1038/nm1144

Mandl, C. W. (2005). **Steps of the tick-borne encephalitis virus replication cycle that affect neuropathogenesis**. *Virus Research*, ***111***(2), 161–174. https://doi.org/10.1016/j.virusres.2005.04.007

Mandl, C. W., Guirakhoo, F., Holzmann, H., Heinz, F. X., & Kunz, C. (1989). **Antigenic structure of the flavivirus envelope protein E at the molecular level, using tick-borne encephalitis virus as a model**. *Journal of Virology*, ***63***(2), 564–571. https://doi.org/10.1128/jvi.63.2.564-571.1989

Mandl, C. W., Kroschewski, H., Allison, S. L., Kofler, R., Holzmann, H., Meixner, T., & Heinz, F. X. (2001). **Adaptation of Tick-Borne Encephalitis Virus to BHK-21 Cells Results in the Formation of Multiple Heparan Sulfate Binding Sites in the Envelope Protein and Attenuation In Vivo**. *Journal of Virology*, ***75***(12), 5627–5637. https://doi.org/10.1128/jvi.75.12.5627-5637.2001

Manokaran, G., Finol, E., Wang, C., Gunaratne, J., Bahl, J., Ong, E. Z., Tan, H. C., Sessions, O. M., Ward, A. M., Gubler, D. J., Harris, E., Garcia-Blanco, M. A., & Ooi, E. E. (2015). **Dengue subgenomic RNA binds TRIM25 to inhibit interferon expression for epidemiological fitness**. *Science*, ***350***(6257), 217–221. https://doi.org/10.1126/science.aab3369

Manzano, M., Reichert, E. D., Polo, S., Falgout, B., Kasprzak, W., Shapiro, B. A., & Padmanabhan, R. (2011). **Identification of Cis-Acting Elements in the 3′-Untranslated Region of the Dengue Virus Type 2 RNA That Modulate Translation and Replication**. *Journal of Biological Chemistry*, ***286***(25), 22521–22534. https://doi.org/10.1074/jbc.m111.234302

Marianneau, P., Steffan, A.-M., Royer, C., Drouet, M.-T., Jaeck, D., Kirn, A., & Deubel, V. (1999). **Infection of Primary Cultures of Human Kupffer Cells by Dengue Virus: No Viral Progeny Synthesis, but Cytokine Production Is Evident**. *Journal of Virology*, ***73***(6), 5201–5206. https://doi.org/10.1128/jvi.73.6.5201-5206.1999

Markoff, L. (2003). **5′- and 3′-noncoding regions in flavivirus RNA**. *Advances in Virus Research*, ***59***, 177–228. https://doi.org/10.1016/s0065-3527(03)59006-6

McGavran, M. H., & White, J. D. (1964). **Electron Microscopic and Immunofluorescent Observations on Monkey Liver and Tissue Culture Cells Infected with the Asibi Strain of Yellow Fever Virus.** *The American journal of pathology*, ***45***(4), 501-517.

McKay, B. E., Molineux, M. L., & Turner, R. W. (2004). **Biotin is endogenously expressed in select regions of the rat central nervous system**. *The Journal of Comparative Neurology*, ***473***(1), 86–96. https://doi.org/10.1002/cne.20109

Meertens, L., Carnec, X., Lecoin, M. P., Ramdasi, R., Guivel-Benhassine, F., Lew, E., Lemke, G., Schwartz, O., & Amara, A. (2012). **The TIM and TAM Families of Phosphatidylserine Receptors Mediate Dengue Virus Entry**. *Cell Host & Microbe*, ***12***(4), 544–557. https://doi.org/10.1016/j.chom.2012.08.009

Miner, J. J., & Diamond, M. S. (2016). **Mechanisms of restriction of viral neuroinvasion at the blood–brain barrier**. *Current Opinion in Immunology*, ***38***, 18–23. https://doi.org/10.1016/j.coi.2015.10.008

Miorin, L., Romero-Brey, I., Maiuri, P., Hoppe, S., Krijnse-Locker, J., Bartenschlager, R., & Marcello, A. (2013). **Three-Dimensional Architecture of Tick-Borne Encephalitis Virus Replication Sites and Trafficking of the Replicated RNA**. *Journal of Virology*, ***87***(11), 6469–6481. https://doi.org/10.1128/jvi.03456-12

Moon, S. L., Anderson, J. R., Kumagai, Y., Wilusz, C. J., Akira, S., Khromykh, A. A., & Wilusz, J. (2012). **A noncoding RNA produced by arthropod-borne flaviviruses inhibits the cellular exoribonuclease XRN1 and alters host mRNA stability**. *RNA*, ***18***(11), 2029–2040. https://doi.org/10.1261/rna.034330.112

Moon, S. L., Dodd, B. J. T., Brackney, D. E., Wilusz, C. J., Ebel, G. D., & Wilusz, J. (2015). **Flavivirus sfRNA suppresses antiviral RNA interference in cultured cells and mosquitoes and directly interacts with the RNAi machinery**. *Virology*, ***485***, 322–329. https://doi.org/10.1016/j.virol.2015.08.009

Nedergaard, M., Ransom, B., & Goldman, S. A. (2003). **New roles for astrocytes: Redefining the functional architecture of the brain**. *Trends in Neurosciences*, ***26***(10), 523–530. https://doi.org/10.1016/j.tins.2003.08.008

Neufeldt, C. J., Cortese, M., Acosta, E. G., & Bartenschlager, R. (2018). **Rewiring cellular networks by members of the Flaviviridae family**. *Nature Reviews Microbiology*, ***16***(3), 125–142. https://doi.org/10.1038/nrmicro.2017.170

Nguyen, N. M., Thi Hue Kien, D., Tuan, T. V., Quyen, N. T. H., Tran, C. N. B., Vo Thi, L., Thi, D. L., Nguyen, H. L., Farrar, J. J., Holmes, E. C., Rabaa, M. A., Bryant, J. E., Nguyen, T. T., Nguyen, H. T. C., Nguyen, L. T. H., Pham, M. P., Nguyen, H. T., Luong, T. T. H., Wills, B., & Simmons, C. P. (2013). **Host and viral features of human dengue cases shape the population of infected and infectious *Aedes aegypti* mosquitoes**. *Proceedings of the National Academy of Sciences*, ***110***(22), 9072–9077. https://doi.org/10.1073/pnas.1303395110

Offerdahl, D. K., Dorward, D. W., Hansen, B. T., & Bloom, M. E. (2012). **A Three-Dimensional Comparison of Tick-Borne Flavivirus Infection in Mammalian and Tick Cell Lines**. *PLOS ONE*, ***7***(10), e47912. https://doi.org/10.1371/journal.pone.0047912

Palus, M., Bílý, T. Š., Elsterová, J., Langhansová, H., Salát, J. Ř., Vancová, M., & Růžek, D. (2014). **Infection and injury of human astrocytes by tick-borne encephalitis virus**. *Journal of General Virology*, ***95***(11), 2411–2426. https://doi.org/10.1099/vir.0.068411-0

Panayiotou, C., Lindqvist, R., Kurhade, C., Vonderstein, K., Pasto, J., Edlund, K., Upadhyay, A. S., & Överby, A. K. (2018). **Viperin Restricts Zika Virus and Tick-Borne Encephalitis Virus Replication by Targeting NS3 for Proteasomal Degradation**. *Journal of Virology*, ***92***(7), e02054-17. https://doi.org/10.1128/jvi.02054-17

Perera-Lecoin, M., Meertens, L., Carnec, X., & Amara, A. (2013). **Flavivirus Entry Receptors: An Update**. *Viruses*, ***6***(1), 69–88. https://doi.org/10.3390/v6010069

Pijlman, G. P., Funk, A., Kondratieva, N., Leung, J., Torres, S., van der Aa, L., Liu, W. J., Palmenberg, A. C., Shi, P.-Y., Hall, R. A., & Khromykh, A. A. (2008). **A Highly Structured, Nuclease-Resistant, Noncoding RNA Produced by Flaviviruses Is Required for Pathogenicity**. *Cell Host & Microbe*, ***4***(6), 579–591. https://doi.org/10.1016/j.chom.2008.10.007

Ponti, D., Troiano, M., Bellenchi, G. C., Battaglia, P. A., & Gigliani, F. (2008). **The HIV Tat protein affects processing of ribosomal RNA precursor**. *BMC Cell Biology*, ***9***(1), 32. https://doi.org/10.1186/1471-2121-9-32

Potokar, M., Korva, M. Š., Jorgačevski, J., Avšič-Županc, T., & Zorec, R. (2014). **Tick-Borne Encephalitis Virus Infects Rat Astrocytes but Does Not Affect Their Viability**. *PLOS ONE*, ***9***(1), e86219. https://doi.org/10.1371/journal.pone.0086219

Presolski, S. I., Hong, V. P., & Finn, M. G. (2011). **Copper-Catalyzed Azide–Alkyne Click Chemistry for Bioconjugation**. *Current Protocols in Chemical Biology*, ***3***(4), 153–162. https://doi.org/10.1002/9780470559277.ch110148

Pulkkinen, L., Butcher, S., & Anastasina, M. (2018). **Tick-Borne Encephalitis Virus: A Structural View**. *Viruses*, ***10***(7), 350. https://doi.org/10.3390/v10070350

Rampersad, S., & Tennant, P. (2018). **Replication and Expression Strategies of Viruses**. *Viruses*, 55–82. https://doi.org/10.1016/b978-0-12-811257-1.00003-6

Rehacek J. (1962). **Transovarial transmission of tick-borne encephalitis virus by ticks**. *Acta Virol*. ***6***, 220-226.

Ray, D., Shah, A., Tilgner, M., Guo, Y., Zhao, Y., Dong, H., Deas, T. S., Zhou, Y., Li, H., & Shi, P.Y. (2006). **West Nile Virus 5′-Cap Structure Is Formed by Sequential Guanine N-7 and Ribose 2′-O Methylations by Nonstructural Protein 5**. *Journal of Virology*, ***80***(17), 8362–8370. https://doi.org/10.1128/jvi.00814-06

Reid, D. W., Campos, R. K., Child, J. R., Zheng, T., Chan, K. W. K., Bradrick, S. S., Vasudevan, S. G., Garcia-Blanco, M. A., & Nicchitta, C. V. (2018). **Dengue Virus Selectively Annexes Endoplasmic Reticulum-Associated Translation Machinery as a Strategy for Co-opting Host Cell Protein Synthesis**. *Journal of Virology*, ***92***(7), e01766-17. https://doi.org/10.1128/jvi.01766-17

Reid, D. W., & Nicchitta, C. V. (2015). **Diversity and selectivity in mRNA translation on the endoplasmic reticulum**. *Nature Reviews Molecular Cell Biology*, ***16***(4), 221–231. https://doi.org/10.1038/nrm3958

Rey, F. A., Stiasny, K., & Heinz, F. X. (2017). **Flavivirus structural heterogeneity: implications for cell entry**. *Current Opinion in Virology*, ***24***, 132–139. https://doi.org/10.1016/j.coviro.2017.06.009

Rice, C., Lenches, E., Eddy, Shin, S., Sheets, R., & Strauss, J. (1985). **Nucleotide sequence of yellow fever virus: implications for flavivirus gene expression and evolution**. *Science*, ***229***(4715), 726–733. https://doi.org/10.1126/science.4023707

Rigby, P. W. J., Dieckmann, M., Rhodes, C., & Berg, P. (1977). **Labeling deoxyribonucleic acid to high specific activity in vitro by nick translation with DNA polymerase I**. *Journal of Molecular Biology*, ***113***(1), 237–251. https://doi.org/10.1016/0022-2836(77)90052-3

Roby, J. A., Hall, R. A., Setoh, Y. X., & Khromykh, A. A. (2015). **Post-translational regulation and modifications of flavivirus structural proteins**. *Journal of General Virology*, ***96***(7), 1551–1569. https://doi.org/10.1099/vir.0.000097

Rostovtsev, V. V., Green, L. G., Fokin, V. V., & Sharpless, K. B. (2002). **A stepwise huisgen cycloaddition process: copper(I)-catalyzed regioselective "ligation" of azides and terminal alkynes**. *Angewandte Chemie (International ed. in English)*, ***41***(14), 2596–2599. https://doi.org/10.1002/1521-3773(20020715)41:14<2596::AID-ANIE2596>3.0.CO;2-4

Roth, H., Magg, V., Uch, F., Mutz, P., Klein, P., Haneke, K., Lohmann, V., Bartenschlager, R., Fackler, O. T., Locker, N., Stoecklin, G., & Ruggieri, A. (2017). **Flavivirus Infection Uncouples Translation Suppression from Cellular Stress Responses**. *MBio*, ***8***(1), e02150-16. https://doi.org/10.1128/mbio.02150-16

Růžek, D., Salát, J. R., Singh, S. K., & Kopecký, J. (2011). **Breakdown of the Blood-Brain Barrier during Tick-Borne Encephalitis in Mice Is Not Dependent on CD8+ T-Cells**. *PLOS ONE*, ***6***(5), e20472. https://doi.org/10.1371/journal.pone.0020472

Salas-Benito, J. S., & del Angel, R. M. (1997). **Identification of two surface proteins from C6/36 cells that bind dengue type 4 virus**. *Journal of Virology*, ***71***(10), 7246–7252. https://doi.org/10.1128/jvi.71.10.7246-7252.1997

Salas-Benito, J., Valle, J. R.-D., Ceballos-Olvera, I., del Angel, R. M., Salas-Benito, M., & Mosso, C. (2007). **Evidence that the 45-kD Glycoprotein, Part of a Putative Dengue Virus Receptor Complex in the Mosquito Cell Line C6/36, Is a Heat-Shock–Related Protein**. *The American Journal of Tropical Medicine and Hygiene*, ***77***(2), 283–290. https://doi.org/10.4269/ajtmh.2007.77.283

Salazar, M. I., Richardson, J. H., Sánchez-Vargas, I., Olson, K. E., & Beaty, B. J. (2007). **Dengue virus type 2: replication and tropisms in orally infected Aedes aegypti mosquitoes**. *BMC Microbiology*, ***7***(1), 9. https://doi.org/10.1186/1471-2180-7-9

Scherbik, S. V., Paranjape, J. M., Stockman, B. M., Silverman, R. H., & Brinton, M. A. (2006). **RNase L Plays a Role in the Antiviral Response to West Nile Virus**. *Journal of Virology*, ***80***(6), 2987–2999. https://doi.org/10.1128/jvi.80.6.2987-2999.2006

Schnettler, E., Sterken, M. G., Leung, J. Y., Metz, S. W., Geertsema, C., Goldbach, R. W., Vlak, J. M., Kohl, A., Khromykh, A. A., & Pijlman, G. P. (2012). **Noncoding Flavivirus RNA Displays RNA Interference Suppressor Activity in Insect and Mammalian Cells**. *Journal of Virology*, ***86***(24), 13486–13500. https://doi.org/10.1128/jvi.01104-12

Schnettler, E., Tykalová, H., Watson, M., Sharma, M., Sterken, M. G., Obbard, D. J., Lewis, S. H., McFarlane, M., Bell-Sakyi, L., Barry, G., Weisheit, S., Best, S. M., Kuhn, R. J., Pijlman, G. P., Chase-Topping, M. E., Gould, E. A., Grubhoffer, L., Fazakerley, J. K., & Kohl, A. (2014). **Induction and suppression of tick cell antiviral RNAi responses by tick-borne flaviviruses**. *Nucleic Acids Research*, ***42***(14), 9436–9446. https://doi.org/10.1093/nar/gku657

Schuessler, A., Funk, A., Lazear, H. M., Cooper, D. A., Torres, S., Daffis, S., Jha, B. K., Kumagai, Y., Takeuchi, O., Hertzog, P., Silverman, R., Akira, S., Barton, D. J., Diamond, M. S., & Khromykh, A. A. (2012). **West Nile Virus Noncoding Subgenomic RNA Contributes to Viral Evasion of the Type I Interferon-Mediated Antiviral Response**. *Journal of Virology*, ***86***(10), 5708–5718. https://doi.org/10.1128/jvi.00207-12

Selinger, M., Tykalová, H., Štěrba, J., Věchtová, P., Vavrušková, Z., Lieskovská, J., Kohl, A., Schnettler, E., & Grubhoffer, L. (2019). **Tick-borne encephalitis virus inhibits rRNA synthesis and host protein production in human cells of neural origin**. *PLOS Neglected Tropical Diseases*, ***13***(9), e0007745. https://doi.org/10.1371/journal.pntd.0007745

Sheth, U., & Parker, R. (2003). **Decapping and Decay of Messenger RNA Occur in Cytoplasmic Processing Bodies**. *Science*, ***300***(5620), 805–808. https://doi.org/10.1126/science.1082320

Shi, P.Y. (2014). **Unraveling a Flavivirus Enigma**. *Science*, ***343***(6173), 849–850. https://doi.org/10.1126/science.1251249

Singh, K. R. P., Pavri, K. H. O. R. S. H. E. D., & Anderson, C. R. (1963). **Experimental Transovarial Transmission of Kyasanur Forest Disease Virus in Haemaphysalis spinigera**. *Nature*, ***199***(4892), 513. https://doi.org/10.1038/199513a0

Sletten, E. M., & Bertozzi, C. R. (2009). **Bioorthogonal Chemistry: Fishing for Selectivity in a Sea of Functionality**. *Angewandte Chemie International Edition*, ***48***(38), 6974–6998. https://doi.org/10.1002/anie.200900942

Slonchak, A., & Khromykh, A. A. (2018). Subgenomic flaviviral RNAs: **What do we know after the first decade of research**. *Antiviral Research*, ***159***, 13–25. https://doi.org/10.1016/j.antiviral.2018.09.006

Slovak, M., Kazimirova, M., Siebenstichova, M., Ustaníkova, K., Klempa, B., Gritsun, T., Gould, E. A., & Nuttall, P. A. (2014). **Survival dynamics of tick-borne encephalitis virus in Ixodes ricinus ticks**. *Ticks and Tick-Borne Diseases*, ***5***(6), 962–969. https://doi.org/10.1016/j.ttbdis.2014.07.019

Sotcheff, S., & Routh, A. (2020). **Understanding Flavivirus Capsid Protein Functions: The Tip of the Iceberg**. *Pathogens*, ***9***(1), 42. https://doi.org/10.3390/pathogens9010042

Stark, G. R., Kerr, I. M., Williams, B. R. G., Silverman, R. H., & Schreiber, R. D. (1998). **How cells respond to interferons**. *Annual Review of Biochemistry*, ***67***(1), 227–264. https://doi.org/10.1146/annurev.biochem.67.1.227

Tan, T. Y., Fibriansah, G., Kostyuchenko, V. A., Ng, T.-S., Lim, X.-X., Zhang, S., Lim, X.-N., Wang, J., Shi, J., Morais, M. C., Corti, D., & Lok, S.-M. (2020). **Capsid protein structure in Zika virus reveals the flavivirus assembly process**. *Nature Communications*, ***11***(1), 895. https://doi.org/10.1038/s41467-020-14647-9

Tassaneetrithep, B., Burgess, T. H., Granelli-Piperno, A., Trumpfheller, C., Finke, J., Sun, W., Eller, M. A., Pattanapanyasat, K., Sarasombath, S., Birx, D. L., Steinman, R. M., Schlesinger, S., & Marovich, M. A. (2003). **DC-SIGN (CD209) Mediates Dengue Virus Infection of Human Dendritic Cells**. *Journal of Experimental Medicine*, ***197***(7), 823–829. https://doi.org/10.1084/jem.20021840

Therkelsen, M. D., Klose, T., Vago, F., Jiang, W., Rossmann, M. G., & Kuhn, R. J. (2018). **Flaviviruses have imperfect icosahedral symmetry**. *Proceedings of the National Academy of Sciences*, ***115***(45), 11608–11612. https://doi.org/10.1073/pnas.1809304115

Troost, B., & Smit, J. M. (2020). **Recent advances in antiviral drug development towards dengue virus**. *Current Opinion in Virology*, ***43***, 9–21. https://doi.org/10.1016/j.coviro.2020.07.009

Urosevic, N., Mansfield, J. P., Shellam, G. R., Mackenzie, J. S., & van Maanen, M. (1997). **Molecular characterization of virus-specific RNA produced in the brains of flavivirus-susceptible and -resistant mice after challenge with Murray Valley encephalitis virus**. *Journal of General Virology*, ***78***(1), 23–29. https://doi.org/10.1099/0022-1317-78-1-23

Vandesompele, J., De Preter, K., Pattyn, F., Poppe, B., Van Roy, N., De Paepe, A., & Speleman, F. (2002). **Accurate normalization of real-time quantitative RT-PCR data by geometric averaging of multiple internal control genes**. *Genome Biology*, ***3***(7), 1-11. https://doi.org/10.1186/gb-2002-3-7-research0034

Venturi, G., Zammarchi, L., Fortuna, C., Remoli, M. E., Benedetti, E., Fiorentini, C., Trotta, M., Rizzo, C., Mantella, A., Rezza, G., & Bartoloni, A. (2016). **An autochthonous case of Zika due to possible sexual transmission, Florence, Italy, 2014**. *Eurosurveillance*, ***21***(8), 30148. https://doi.org/10.2807/1560-7917.es.2016.21.8.30148

Verma, S., Kumar, M., & Nerurkar, V. R. (2010). **Cyclooxygenase-2 inhibitor blocks the production of West Nile virus-induced neuroinflammatory markers in astrocytes**. *Journal of General Virology*, ***92***(3), 507–515. https://doi.org/10.1099/vir.0.026716-0

Villordo, S. M., Carballeda, J. M., Filomatori, C. V., & Gamarnik, A. V. (2016). **RNA Structure Duplications and Flavivirus Host Adaptation**. *Trends in Microbiology*, ***24***(4), 270–283. https://doi.org/10.1016/j.tim.2016.01.002

Vonderstein, K., Nilsson, E., Hubel, P., Nygård Skalman, L., Upadhyay, A., Pasto, J., Pichlmair, A., Lundmark, R., & Överby, A. K. (2017). **Viperin Targets Flavivirus Virulence by Inducing Assembly of Noninfectious Capsid Particles**. *Journal of Virology*, ***92***(1), e01751-17. https://doi.org/10.1128/jvi.01751-17

Vreede, F. T., & Fodor, E. (2010). **The role of the influenza virus RNA polymerase in host shut-off**. *Virulence*, ***1***(5), 436–439. https://doi.org/10.4161/viru.1.5.12967

Wei, C.-M., Gershowitz, A., & Moss, B. (1975). **Methylated nucleotides block 5′ terminus of HeLa cell messenger RNA**. *Cell*, ***4***(4), 379–386. https://doi.org/10.1016/0092-8674(75)90158-0

Welsch, S., Miller, S., Romero-Brey, I., Merz, A., Bleck, C. K. E., Walther, P., Fuller, S. D., Antony, C., Krijnse-Locker, J., & Bartenschlager, R. (2009). **Composition and Three-Dimensional Architecture of the Dengue Virus Replication and Assembly Sites**. *Cell Host & Microbe*, ***5***(4), 365–375. https://doi.org/10.1016/j.chom.2009.03.007

Wichapong, K., Pianwanit, S., Sippl, W., & Kokpol, S. (2010). **Homology modeling and molecular dynamics simulations of Dengue virus NS2B/NS3 protease: insight into molecular interaction**. *Journal of Molecular Recognition*, ***23***(3), 283–300. https://doi.org/10.1002/jmr.977

Ye, J., Zhu, B., Fu, Z. F., Chen, H., & Cao, S. (2013**). Immune evasion strategies of flaviviruses**. *Vaccine*, ***31***(3), 461–471. https://doi.org/10.1016/j.vaccine.2012.11.015

Yu, I.-M., Zhang, W., Holdaway, H. A., Li, L., Kostyuchenko, V. A., Chipman, P. R., Kuhn, R. J., Rossmann, M. G., & Chen, J. (2008). **Structure of the Immature Dengue Virus at Low pH Primes Proteolytic Maturation**. *Science*, ***319***(5871), 1834–1837. https://doi.org/10.1126/science.1153264

Zakaria, M. K., Carletti, T., & Marcello, A. (2018). **Cellular Targets for the Treatment of Flavivirus Infections**. *Frontiers in Cellular and Infection Microbiology*, ***8***, 398. https://doi.org/10.3389/fcimb.2018.00398

Zhang, X., Xie, X., Xia, H., Zou, J., Huang, L., Popov, V. L., Chen, X., & Shi, P.-Y. (2019). **Zika Virus NS2A-Mediated Virion Assembly**. *MBio*, ***10***(5), e02375-19. https://doi.org/10.1128/mbio.02375-19

Internet sources

1. https://www.thermofisher.com/document-connect/document-connect.html?url=https%3A%2F%2Fassets.thermofisher.com%2FTFS-Assets%2FLSG%2Fmanuals%2Fpcdnadest40_man.pdf&title=cGNETkEtREVTVDQwIEdhdGV3YXkgVmVjdG9y

2. https://www.jenabioscience.com/images/741d0cd7d0/bro_Click_labeling_cellular_metabolites.pdf

3. https://www.thermofisher.com/document-connect/document-connect.html?url=https%3A%2F%2Fassets.thermofisher.com%2FTFS-Assets%2FLSG%2Fmanuals%2FMAN0011280_DTSSP_DSP_UG.pdf&title=VXNlciBHdWlkZTogIERUU1NQIERTUA==